

Article

Bottle Emptying: A Fluid Mechanics and Measurements Exercise for Engineering Undergraduate Students

Hans C. Mayer

Department of Mechanical Engineering, California Polytechnic State University, San Luis Obispo, CA 93407, USA; hmayer@calpoly.edu

Received: 12 September 2019; Accepted: 30 September 2019; Published: 11 October 2019



Abstract: A comprehensive exercise, suitable for an undergraduate engineering audience studying fluid mechanics, is presented, in which participants were tasked with emptying a bottle. That simple request yielded data collected by students and the author for $N = 454$ commercially available bottles, spanning nearly four orders of magnitude for volume \mathcal{V} , and representing the largest experimental dataset available in the literature. Fundamental statistics are used to describe the emptying time, \bar{T}_e , for any single bottle. Dimensional analysis is used to transform the raw data to yield a predictive trend, and a method of least-squares regression analysis is performed to find an empirical correlation relating dimensionless time $\bar{T}_e \sqrt{g/d}$ and dimensionless volume \mathcal{V}/d^3 . We find that volume, \mathcal{V} , and neck diameter, d , can be used to estimate the emptying time for any bottle, although the data suggests that the shape of the neck plays a role. Furthermore, two basic analytical models found in the literature compare favorably to our data and empirical correlation when recast using our dimensionless groups. The documented exercise provides students with the opportunity to use basic engineering statistics and to see the utility of dimensional analysis.

Keywords: multiphase flow; slugging; flooding; bottle; bubbles

1. Introduction

1.1. A Familiar Scene

The scene depicted in Figure 1a is a familiar one. Here, we see a sequence of still images, captured during the emptying of an inverted bottle, that show the complex behavior of water leaving and air entering through the single opening at the neck. When we observe such an emptying event in its entirety, we cannot help but marvel at what unfolds—in particular, the violent motion within the bottle as rising bubbles reach the surface and the oscillatory flow at the outlet, all of which is accompanied by a series of “glugs” until at last the bottle has been evacuated. We do our best to illustrate this behavior in the superposition of sequenced images in Figure 1b, which from start to finish takes ~ 10 s. The images of Figure 1c present a strikingly different scene. Here, we have removed the bottom of the bottle, and we now find the flow to be orderly and predictable, without the competition between fluid phases at the neck. This emptying process takes only ~ 2 s, Figure 1d showing the superposition of images and progression of the surface. Thus, if we ask, “what is the emptying time for a bottle?” The answer is readily accessible for the vessel of Figure 1c,d, but can be a daunting task for that of Figure 1a,b, in particular for an undergraduate engineering student at the start of their study of fluid mechanics.

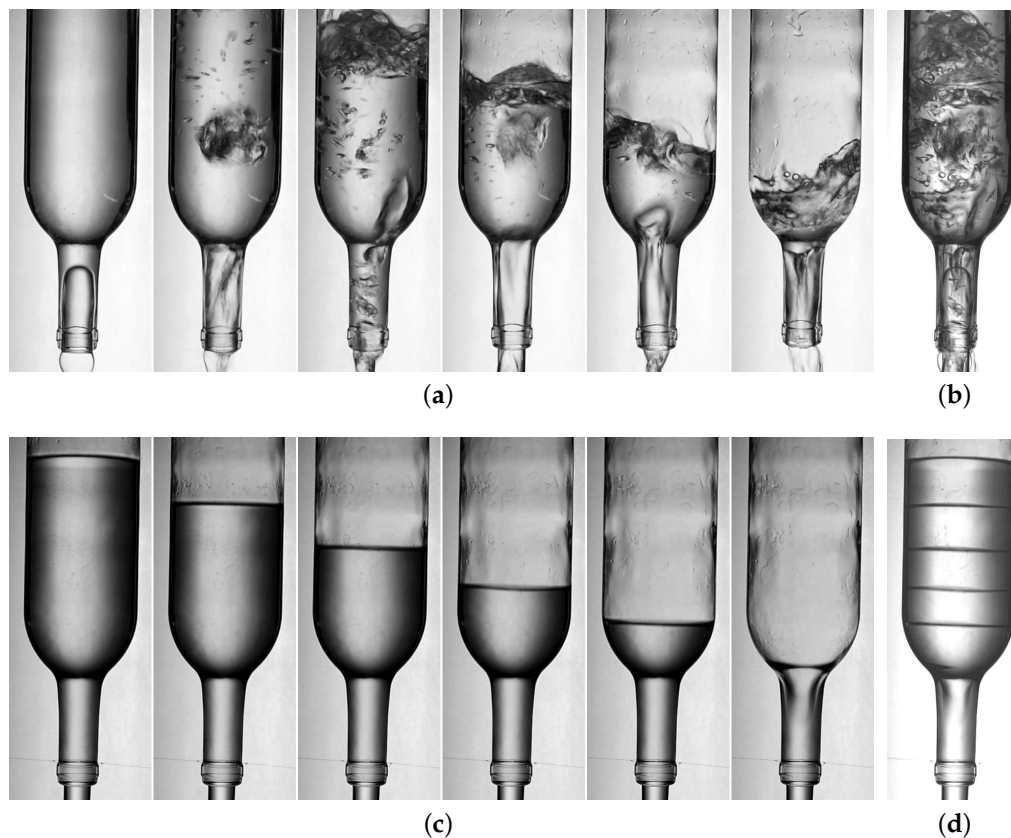


Figure 1. Photographs of water emptying from a bottle (wine bottle: 750 mL volume and 20 mm diameter opening at neck). (a) A sequence of images from the emptying event (1.67 s apart). A slug of air can be seen to exist in the neck and the bulk of the liquid is populated with bubbles both large and small. Superposition of sequential images during a typical emptying event is shown in panel (b). When the bottom of the bottle is removed, making it an open-top container when inverted, the scene in panel (c) is strikingly different (0.23 s between images). The air–water interface within the bottle is flat, its position more readily predictable (d), and has a uniform jet of liquid issues from the opening in the neck rather than a behavior. All images were recorded at 60 fps using a Nikon D3400.

1.2. Literature Review

The complexity of bottle emptying, as exemplified in Figure 1, must have casually intrigued scientists and laypersons for a very long time, but a review of the literature only shows a handful of papers dedicated to the scientific study of the subject, and these were published primarily over the last three decades. Although Davies & Taylor [1] and Zukoski [2] investigated the drainage of tubes via the passage of long bubbles, Whalley [3,4] was the first to investigate the emptying times of real bottles, i.e., commercially available bottles characterized by a neck with a diameter smaller than that of the body. His studies were concerned with the overall emptying time of these vessels, which ranged in size and shape, and he recognized that the total time was governed by the nature of the flow at the outlet—in particular, he identified the closely related phenomena of flooding and slugging and their relation to this flow. The occurrence of flooding, a type of concurrent flow of gas and liquid phases within a tube, can be predicted using a semiempirical relation attributed to Wallis [5] that incorporates a Wallis flooding “constant” C (see Section 2.5). For an air–water system, this results in values of $C \sim \mathcal{O}(1)$. The values of C calculated from the experiments of Whalley, using a small number of bottles, yielded consistent results strengthening the idea that bottle emptying is a flooding process. Furthermore, Whalley recognized that emptying is also similar to slugging: another regime of two-phase flow in which large slugs of gas form in tubes. If thought of in this context, the emptying process can be modeled as liquid flowing out of the bottle and around a stationary slug of air (cf. Figure 1b, looking

closely at the bottleneck). Whalley's experiments also demonstrated that emptying time, and thus C , can be influenced by water temperature, neck length (artificially created using tube inserts), and angle of inclination. He further considered differences between bottle emptying and filling, the later process was accomplished by submerging an upright empty bottle below the free surface of water in a large tank. Tehrani [6] also measured the emptying time for a very limited number of bottles and found, similar to the results of Whalley, that increases in water temperature significantly influence emptying time.

More rigorous experiments concerning the emptying of bottles were undertaken by Schmidt and Kubie [7], but to carefully investigate the details of emptying, they performed controlled experiments with "ideal" bottles, i.e., various sizes of plastic tubes of constant cross section with centrally located outlets that provided short necks (with either sharp or filleted/profiled entrances). These authors recognized the cyclical nature of the emptying process, but were concerned primarily with gross behavior of the air–water interface within the body of the bottles and not the physics of the process on the single-cycle scale. In particular, their key findings showed that during emptying the velocity of the air–water interface (within the bottle) is nearly constant with respect to the level in the bottle, implying that height does not play a role in the total emptying time beyond increasing the volume of the container; that the velocity changes with the shape of the outlet (increasing velocity with more rounded entrances); and that the average liquid discharge velocity increase weakly with both bottle diameter and neck diameter. These key results were echoed in the findings of Kordestani and Kubie [8] and Tang and Kubie [9], who also used "ideal" bottles. Unlike Schmidt and Kubie, Kordestani and Kubie presented many of the results of their experiments in the form of the Wallis flooding constant C and found favorable comparison to the results of Whalley (cf. Section 2.5), noting that C increases with a smoother outlet profile (increasing C indicating a faster emptying time). Their experiments with liquids emptying from bottles into a liquid environment demonstrated that the nature of the emptying process is the same but slower than the gas–liquid case. Changes in C for air–water systems due to the inclination of the outlet was investigated by Tang & Kubie [9].

Clanet & Searby [10], without reference to the multiple works of Whalley [3,4] or Kubie [7–9], thoroughly investigated the emptying of ideal bottles both theoretically and experimentally, considering both the long timescale associated with complete emptying and the short timescale responsible for the familiar "glug-glug". The basic construction of their bottles was the same as that of Kubie et al., i.e., long tubes with centrally-located outlets; however, Clanet and Searby used thin plates with sharp edges for their outlets rather than the thicker plates of Kubie. Not surprisingly, owing to the similarity in apparatus, their experiments revealed the same quasi-constant velocity of the air–water interface within the tube and noted that this velocity decreased with reduction in outlet diameter. These authors also developed a simple analytical model to predict the emptying time for these bottles which we will make use of later. Considerable detail is provided by Clanet & Searby regarding the physical origin of the oscillations (in mass flow rate and pressure) characterizing the short timescale glug-glug, but those results are not directly relevant to the new work presented here. Most recently, computational fluid dynamics (CFD) has been shown by Geiger et al. [11] to accurately simulate the bottle emptying process, including the transient behavior of the complex two-phase flow and the overall emptying time. A CFD analysis of bottle emptying has also been published by Mer et al. [12], along with experiments to quantify transient and oscillatory behavior associated with the variety of two-phase flow phenomenon encountered during emptying [13]. These experimental results are expected to help validate future CFD studies.

1.3. Motivation—Establishing a Curricular Thread

Inspiration for the elements of this paper originated from a homework problem buried within S. Middleman's "Introduction to Fluid Dynamics" [14], which begins "a classroom demonstration on the time to drain water from a set of initially filled inverted bottles yielded the following results. . ." and is concluded with a set of six data points (bottle volume and emptying time) extracted from

the work of P.B. Whalley [4]. Expanding on this example, we have developed a complete exercise that provides the opportunity for a class of students to consider a complex, but commonplace, fluid flow phenomenon from the standpoint of dimensional analysis; collect and analyze data using basic engineering statistics; combine data to form a large set; plot the data; and extract a predictive trend using basic regression techniques. Such an exercise, presented as a complete unit, forms what might be considered a curricular thread, stitching together various aspects of a variety of science and engineering courses, in particular an undergraduate fluid mechanics course. However, as the emphasis of the exercise is not a detailed investigation of the fluid dynamics of a multiphase flow, the exercise described here is accessible to a broad audience and would be of value beyond a fluid mechanics course. Furthermore, because of the nature of the experiments, there is no need for expensive laboratory equipment or an elaborate demonstration apparatus—a plethora of bottles in a wide variety of shapes and sizes are readily available. In addition, the instructions for data collection are simple, and as such give the project a feel of a public study [15]. This particular fluid mechanics example has the added advantage that the data can be compared directly to a select number of sparse datasets. If an instructor is so inclined, there also exists the opportunity to encourage students to research the open literature for the two models provided for comparison. In doing so, they will find evidence of the rich and complex phenomena that accompany an event that might previously have been considered mundane. In what follows, we present this complete exercise and results from data collected by students and the author, over many academic quarters and years, who were asked a simple but intriguing question: “What is the emptying time for a bottle?”

1.4. Outline

The work presented here is divided conveniently into several main parts. In Section 2.1, we introduce the protocol for data collection. In Section 2.2, an analysis of the basic statistics associated with the data obtained from a few single bottles is presented. A complete picture of the emptying time data for the entire collection of bottles is contained in Section 2.3 as well as a summary of the measurement uncertainties from experiments. A review of the dimensional analysis used to obtain relevant dimensionless groups is presented ending with a graphical summary of that analysis. In Section 2.4, we focus on regression analysis of the dimensionless data to obtain a predictive trend for bottle emptying. Finally, in Section 2.5, we compare our data and the results from the regression analysis to the limited bottle emptying data available in the literature. We also provide comparisons of simple models published in the literature to our extensive dataset and find reasonable agreement.

The primary audience for this paper are instructors and students in an undergraduate engineering fluid mechanics course; however, the data by itself would be useful in an engineering statistics/measurements course. The paper is structured so that different portions can be used to direct exercises in those topics. For example, Sections 2.2 and 2.4 can be considered as standalone projects for an engineering statistics class, whereas Sections 2.3 and 2.5 are suited for a dimensional analysis example or homework problem in a fluid mechanics lecture. Alternatively, all aspects (Sections 2.2–2.5) together form a complete investigation and represent a project that when applied at the appropriate level leverages content from a variety of engineering courses.

2. Results and Discussion

What follows is a suggested presentation of the data and analysis for use as a student exercise and/or guided discussion. It is intended for an undergraduate engineering audience. Familiarity with basic statistics and fluid mechanics are helpful; however, sufficient details, guidance, and references have been provided for the reader. All quantitative analysis can be completed using a basic computer spreadsheet program, e.g., Excel[®], or programmed in MATLAB[®], and do not require any statistics-specific software. All experiments can be completed using simple tools and instruments (e.g., a stopwatch, ruler, graduated cylinder, scale, etc.). Components of the complete exercise presented here

were implemented in various forms during sophomore or junior level classes at California Polytechnic State University San Luis Obispo, the University of California at Santa Barbara, and Rutgers University.

2.1. Data Collection Protocol

Regardless of the format of the exercise (e.g., an extended statistics-only exercise, a fluid mechanics dimensional analysis problem, or both), students were provided with a basic data sheet and a short handout explaining the overall goal—to gain insight into emptying of single outlet vessels via collective experiments using commercially available bottles. Each student was tasked with finding a bottle or single-outlet container for their experiment (from here on the term “bottle” will be used exclusively to denote any single-outlet container used for experiments). Certain limitations applied: ordinary soda/beer bottles were discouraged to promote a wide variety of shapes and sizes (no restriction was placed on the shape), and it was suggested that the bottles be rigid (e.g., glass or hard plastic) to reduce, or avoid altogether, flexing of the sidewalls during emptying. Because the interest is in single-outlet containers, students were encouraged to use any single-outlet vessel. Thus, many of the “bottles” collected for use were not intended for drinking or even holding liquids. Examples include bottles for cooking sauces and oils, jars, soap/shampoo bottles, vases, etc.

Once a bottle was found, students were asked to measure the internal neck diameter, d , and report the nominal value and the measurement uncertainty (further details are provided in Section 2.3 where relevant). Measurements of internal bottle volume V were performed gravimetrically or volumetrically as permitted by availability of equipment. Students were instructed to fill the bottle completely for these internal volume measurements, as all emptying experiments would use filled bottles. Gravimetric measurements were performed using digital balances, and volumetric measurements were obtained using graduated cylinders, measuring cups, or syringes. In all cases, a nominal value and measurement uncertainty for the bottle volume was obtained. Later versions of student instructions asked for measurements of overall bottle height, H , and maximum diameter, D , along with a reporting of the measurement uncertainties. The later inclusions of bottle height and maximum diameter mean that there are more measurements of emptying time that correspond to values of d and V than those that correspond to d , V , H , and D . In these later iterations, students were also asked to submit photographs of bottles to confirm shapes and reported dimensions.

A simple data collection protocol was followed. To start, the bottle was completely filled (up to the outlet of the neck) with room temperature tap water, assuring approximate consistency in liquid viscosity and surface tension. Next, the bottle opening was blocked with a hand or card to prevent outflow and then the bottle was inverted and oriented vertically. Inversion was followed by a short delay to minimize swirl during emptying. It is known that emptying time for bottles will vary with the orientation angle as well as swirl [4]. The protocols students were asked to follow attempt to reduce the effect of both variables from the experimental results. Finally, the students let the bottle empty while recording the overall emptying time T_e . This process was repeated for $n = 3, 5, 10$, or 25 trials depending on the theme of the exercise and/or difficulty in handling filled bottles (this is especially true for very large bottles, i.e., of several gallons, where $n = 3-5$ was considered reasonable).

Not surprisingly, the students participating in these exercises were able to find a diverse range of bottle shapes and sizes. Several hundred students, distributed over multiple academic quarters, have contributed to the bottle emptying data presented here, along with many bottles and containers tested by the author. The result is that for the present study we have data from $N = 454$ bottles (The entire $N = 454$ collection of bottle information, including the dimensions (d , D , H , and V), shape designation, and emptying times, are available in Table S1 in the Supplementary Materials section). Efforts have been made to reduce to an insignificant number duplicate bottles from this dataset. This was accomplished by either a direct visual examination of the bottle (to assess shape, brand, etc.) or a review of a photograph provided by the student. This dataset is larger than any other reported in the literature [3,4,6] and represents a vast range of shapes and sizes. In particular, bottle volume spans $10 \lesssim V \lesssim 27,000$ mL, with emptying times ranging from less than a second to nearly four minutes.

2.2. Exercise 1—Single Bottle Experiments (Statistics Focus)

This section provides an overview of statistics generated from multiple measurements of emptying time using a single variable, e.g., descriptive statistics and basic inferential statistics based on the emptying time considered as a normally distributed variable. Several graphical means of describing the data are also presented. A complete listing of equations used to generate the reported statistics is found in Appendices A and B. We start here, before proceeding to the results, using dimensional analysis, as this could be treated as a standalone exercise in basic statistics.

2.2.1. Single Bottle Statistics—Descriptive

The data and analysis from experiments performed by the author is now provided, in which a single bottle was emptied 100 times. When students were asked to perform similar experiments for the purpose of single bottle statistics, the number of trials was reduced to 10–25 in the interest of limiting experimentation time outside of class. However, larger number of trials are preferable from the standpoint of obtaining statistically significant results. Here, the measurand of interest is the emptying time, T_e . As demonstrated in what follows, data collected from a single bottle can be used to introduce and/or reinforce the key elements of descriptive statistics, graphical presentation of data, and basic inferential statistics for a single variable. Later, we show how these findings are used to estimate overall emptying time uncertainty.

Before considering in detail the data collected during the course of experiments, it is worthwhile to generate a sequential plot to ensure that the emptying time does not itself change with time/order, i.e., to ensure that time is not a lurking variable [16] in the analysis that follows (although it is not anticipated, based on the physics of bottle emptying, that the emptying time will vary with the order of collection). Pedagogically, this is an instance in which, prior to generating the plot, students can reflect on what they expect to see from a sequential plot of the data and explain their expectations. Figure 2a depicts the sequential plot of bottle emptying time for 100 trials performed with the same bottle (cf. Figure 7a for a diagram of the bottle). The data appears as expected, possessing a time-invariant central tendency and spread, quantified later, with the scatter in the data likely caused by subtle differences in the initial conditions of the experiment, for example, differences in filled volume, initial fluid motion within the bottle, and geometry of the air–water interface at the bottle opening. Reaction time likely plays a role as well. We can therefore proceed with further analysis and turn our attention to descriptive statistics and graphical presentations of those results.

At this point, we make no assumption regarding the distribution of the data, nor do we make any inference from the data. Rather, we are interested in providing concise summary measures of the data at hand [16]. The summary measures of interest will describe the central tendency of the data, the spread—or variability—about the central tendency, and the shape of the data. More specifically, these measures will be the sample mean, median, sample standard deviation, five-number summary, and the skewness and kurtosis. We can also graphically present the data to highlight these metrics.

The mean (A1) is easily calculated using a spreadsheet, and for the data shown in Figure 2a, the mean value is $\bar{T}_e = 6.61$ s. The median—the middle value in the ordered set of data—is $\tilde{T}_e = 6.63$ s. A difference of only 0.3% exists between the two measures of the central tendency. There are many ways to characterize the spread, or variability, of the data about the measure of the central tendency. We will begin by generating a “five-number summary” after the data has been ordered from minimum to maximum (j will be the index for the ordered dataset). Once ordered, we can easily obtain the range $T_{e,\max} - T_{e,\min}$, and the interquartile range, i.e., $IQR = Q_3 - Q_1$, where Q is used to denote a quartile. The complete five-number summary is presented in Table 1.

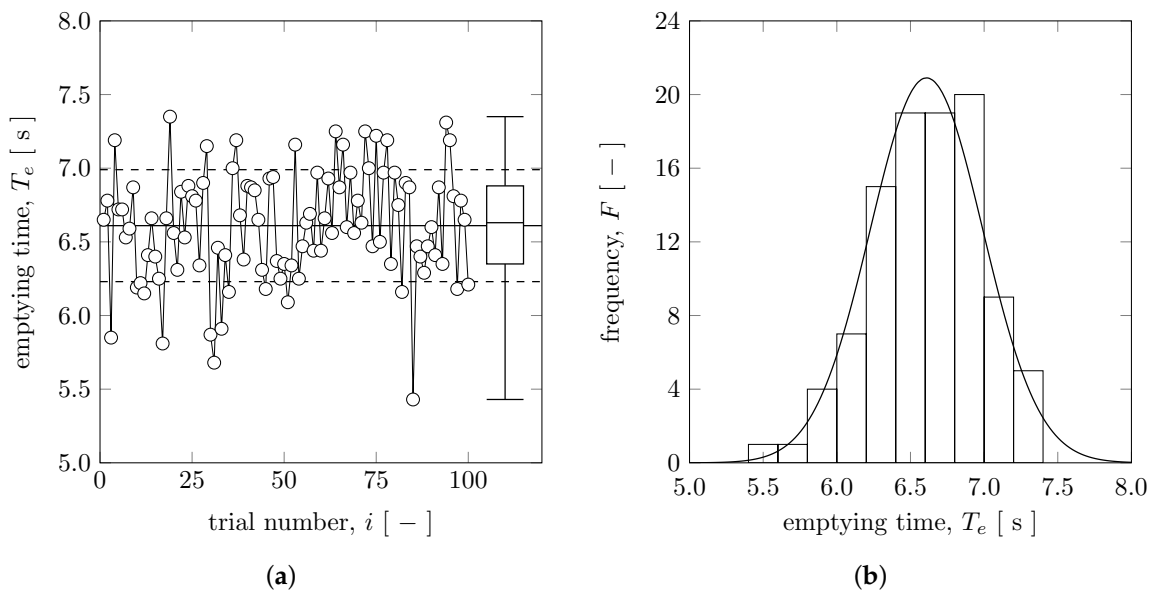


Figure 2. (a) Sequential plot of emptying time recorded from 100 trials using a single bottle (Brer Rabbit Molasses, 375 mL, and $d = 18.3$ mm; cf. Figure 7a). Emptying time was measured using a digital stopwatch with 0.01 s resolution. No apparent trend over time (i.e., trial number i) is suggested by the plot. The sample mean ($\bar{T}_e = 6.61$ s) is shown as the solid horizontal line, and the sample standard deviation ($s = 0.38$ s) is indicated symmetrically about the mean by the dashed lines. Counting of the data points reveals that 71% are located within $\bar{T}_e \pm s$. A box-and-whisker plot is located at the right edge. The extent of the box is reflective of the interquartile range and the line within the box indicates the value of the median ($\tilde{T}_e = 6.63$ s). (b) Frequency distribution created from the single bottle data ($n = 100$). For the distribution shown, the bin number is $k = 10$ and $\Delta T_e = 0.20$ s. Superimposed on the histogram is a normal distribution generated using \bar{x} and s , in place of μ and σ within Equation (A8), and it is evident that there is agreement.

Table 1. The five-number summary for the single bottle data collected by the author ($n = 100$).

Summary Item	j [-]	Value [s]	IQR [s]	Range [s]
$T_{e,\min}$ (minimum)	$j = 25$	5.43		
Q_1 (1st quartile)	$j = 25$	6.35		
\tilde{T}_e (median)	$j = 50/51$	6.63	0.53	1.92
Q_3 (3rd quartile)	$j = 76$	6.88		
$T_{e,\max}$ (maximum)	$j = 100$	7.35		

The five-number summary can be depicted graphically in the form of the box-and-whisker plot [16]. This type of plot is provided on the right edge of Figure 2a. The shape of the box-and-whisker plot reinforces the notion that the distribution of emptying times measured for a single bottle is nearly symmetric. Aside from the five-number summary, we can calculate a single value to characterize the spread, namely, the sample standard deviation s (A2), which for the data has a value of $s = 0.38$ s. The standard deviation can be considered as a kind of “average” distance the data sits, as a whole, from the central tendency. The extent of the standard deviation about the sample mean, i.e., $\bar{T}_e + s$ and $\bar{T}_e - s$, is also shown in Figure 2a, and we find that 71 out of 100 data points, i.e., 71%, fall within this region.

The symmetry and peakedness of the measurand distribution, both measures of the shape, can each be expressed by a single value—the skewness Sk (A3) and kurtosis Ku (A4), respectively. We find, for the data in Figure 2a, the value of the skewness to be $Sk = -0.34$ and the kurtosis $Ku = 3.03$. Skewness can take on both positive and negative values. Positive skewness implies a distribution shape

that is shifted to the right, or, more specifically, the mean value exceeds the mode. Negative skewness indicates the reverse—the value of the mode exceeds the mean. For a symmetric distribution, $Sk = 0$, i.e., the mean value is equal to the mode value [17]. To interpret the value of the skewness obtained from our data, let us consider the following rules of thumb [18]; highly skewed, $|Sk| > 1$; moderately skewed, $1 > |Sk| > 0.5$; approximately symmetric, $0.5 > |Sk|$. Using this interpretation with a value of $Sk = -0.34$, we can conclude that the distribution is approximately symmetric. The kurtosis calculated from a set of data is often compared against the value for a known distribution, the normal distribution being a frequent comparator. For a normal distribution, $Ku = 3$, with values of $Ku < 3$ representative of a flatter distribution, and values of $Ku > 3$ for more peaked distributions [17]. Therefore, the calculated value for the kurtosis ($Ku = 3.03$) is reasonably close to that of a normal distribution. It should not be surprising then that we found 71% of the data to fall within $\bar{T}_e \pm s$, as 68% of data will fall within $\mu \pm \sigma$ for a normal distribution (and for $n = 100$ we expect that $\bar{x} \rightarrow \mu$ and $s \rightarrow \sigma$; in other words, the sample is approaching a population).

The quantitative measures of the central tendency, spread, and shape can also be graphically presented, as we have seen with the sequential plot and box-and-whisker plot. However, a frequency distribution (i.e., histogram) more clearly illustrates the mode and shape, and it is worth developing one here. Later, we will use this histogram from our experimentally determined data to support the selection of a standard probability density function, so as to further interpret the data.

For the student, it is important to recognize the bin number (or number of classes), k , should be selected to adequately convey the nature of the distribution of data. Little can be learned from a histogram with too many or too few bins [16]. Although the development of a histogram can be highly subjective—the selection of bin number and boundaries is at the discretion of the student—there are a few rules of thumb to consider: (1) in general [19], the bin number should be some value between 5–20; (2) for $n > 40$, consider using $k = 1.87(n - 1)^{0.4} + 1$ as a starting estimate [20]; and (3) for large enough n , try $k \sim \sqrt{n}$ as an initial estimate [21]. Regardless of method, one should take care to consider the resolution with which the measurand was obtained, as this can influence the frequency of values contained in bins as the value of k gets large with increasing n , i.e., bin sizes smaller than the resolution of the measuring instrument can lead to artificially empty bins.

For $n = 100$, the rules of thumb suggest that $k = 10$ or 13 will be reasonable. Using the value of the range (cf. Table 1), this yields bins with widths of 0.20 and 0.15 s. The data from Figure 2a was binned using $k = 10$, and the frequency F of occurrences in each bin was tabulated. The result is shown in Figure 2b, and the distribution demonstrates that the data is unimodal and approximately symmetric (consistent with the calculated value of Sk and the box-and-whisker plot shape).

2.2.2. Single Bottle Statistics—Inference

In the previous section, we did not utilize a standard distribution to interpret the data; we simply described the data quantitatively and graphically. However, the purpose of obtaining a sample set of emptying times is to ultimately develop an estimate of the “true” emptying time for any particular bottle in the complete set of $N = 454$, i.e., an estimate of the population mean including a statistical uncertainty (which will be combined with a measurement uncertainty). This will be used in later portions of this work when the results of different bottles are used collectively.

The evidence presented thus far suggests that the emptying times are, or can be modeled as being, normally distributed. Specifically, the skewness $Sk = -0.34$ (near zero) implies the distribution is approximately symmetric, and the kurtosis $Ku = 3.03$ suggests the distribution is near-normal; the number of data points contained within $\bar{T}_e \pm s$ and the frequency distribution of Figure 2b hint at the characteristic Gaussian shape. If the assumption that emptying times are normally distributed is valid, then with the data from a sample, we can estimate the population mean using $T_{e,\mu} = \bar{T}_e \pm [(t_{\nu}s) / \sqrt{n}]$, where the μ subscript implies a population parameter and the degrees of freedom is expressed as $\nu = n - 1$. The Student- t variable t_{ν} is tabulated and is a function of the degrees of freedom and

percent confidence specified [21]. The sample mean and sample standard deviation have already been calculated; to utilize this estimate we must clearly demonstrate normalcy in the data.

To supplement the evidence, we can strengthen the visual assessment of normalcy in two ways. The first involves superimposing atop the data from Figure 2b a continuous curve representing a normal frequency distribution. We can generate such a curve by starting with the probability density function for a normally distributed variable (see Appendix B). Recalling that the probability density p can be related to the relative frequency f and therefore the frequency F for a finite sample, we can create the normal distribution $F(T_e)$. Added to the frequency distribution in Figure 2b is the continuous curve representing a normal distribution. A visual inspection of Figure 2b shows that the frequency distribution for the data is consistent with the shape of a normal distribution.

A second graphical method to evaluate the normalcy of data is the normal probability plot. This is a plot of the standard normal variable, z , versus the measurand, i.e., T_e . Each value of z is obtained by assigning every ordered data point an equal cumulative probability and then calculating the corresponding value of z based on the cumulative probability, assuming that the data is normally distributed. Specific details for developing the plot can be found in standard statistics textbooks [16,21]. The purpose of the normal probability plot is that if the data is approximately normal, the plot of z vs. T_e will be linear according to the definition of the standard normal variable, i.e., $z = (T_e - \mu) / \sigma$. Therefore, rather than relying on a comparison of curved shapes as in Figure 2b, we can visually inspect how the data falls against a straight line. A normal probability plot for the bottle emptying data is given in Figure 3a along with a straight line to guide eye. This graphical assessment of normalcy is reasonable if there at least 20 data points [16], as is the case here ($n = 100$), and under conditions when students are asked to perform 25 measurements (e.g., if the instructor is intending to emphasize the statistics aspect of this exercise). The majority of the points in Figure 3a fall along the straight line and would pass a “fat pencil test”, with only a few points at the upper and lower tails showing deviation. Little weight is placed on the extreme points if they fail to fall along the straight line [21].

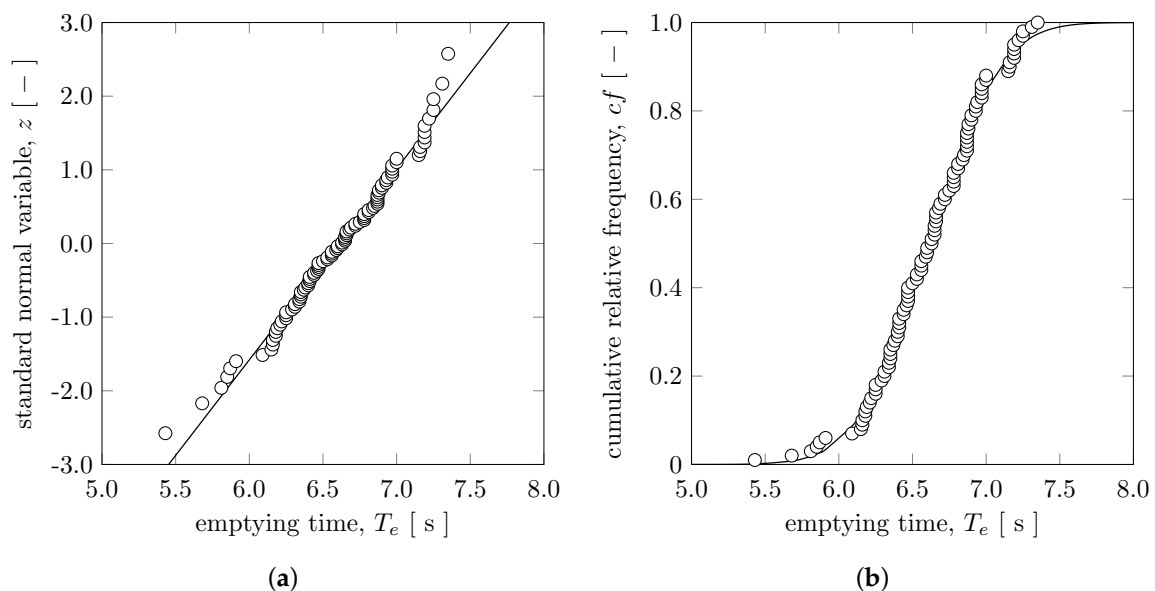


Figure 3. (a) A normal probability plot and (b) a cumulative relative frequency plot of the bottle emptying time data. The normal probability plot, z vs. T_e , shows a linear relationship between the two variables, with the exception of a few data points contained in each of the tails. Typically, little emphasis is placed on the agreement of data in the tails [21]. This linear trend is indicative of data that can be considered normally distributed for the purposes of inference.

Lastly, a final quantitative justification for treating the bottle emptying time as being normally distributed can be had by determining whether or not the empirical distribution when compared to a normal distribution passes the Kolmogorov–Smirnov test, cf. Appendix B and Equation (A9). This involves comparing the maximum deviation between the empirical cumulative frequency and the cumulative frequency for a continuous normal distribution. For the $n = 100$ points, the maximum deviation was found to be $d_{KS} = 0.043$, which is below the critical value of $d_{\alpha}(n) = 0.136$ for a level of confidence of $\alpha = 0.05$. This indicates that the normal distribution passes the Kolmogorov–Smirnov test. A visual comparison of the empirical cumulative frequency and the theoretical normal cumulative frequency can be found in Figure 3b.

In summary, the collective evidence presented in this section suggests that bottle emptying times can be reasonably modeled as normally distributed, for the sake of estimating the population mean for emptying time. Thus, using Equation (A5), we can determine that the emptying time for this particular bottle, accounting for the statistical uncertainty is $T_{e,\mu} = 6.61 \pm 0.08$ s (with 95 % confidence).

2.2.3. Single Bottle Statistics—Additional Examples

Given the many academic quarters that the author has used this exercise, there have been numerous instances in which the same type of bottle has been used by students for data collection. Although these redundant sets of data are not included in the sections that follow (where we attempt to use unique bottles for each data point), here they present the opportunity to show that a similar presentation of single bottle statistics (descriptive and inferential) can be had, without subjecting one experimenter to the tedious task of emptying a bottle 100 times. Examples of data collected by multiple students using the same type of bottles is shown in Figure 4. Within Figure 4a we see sequential plots and box-and-whisker plots for three different bottles (milk, tea, and soda). Figure 4b shows the corresponding histograms and normal distributions. Again, the data suggests that bottle emptying time can be reasonably modeled as normally distributed. Perhaps the only distinct feature of Figure 4a as compared to Figure 2a are instances of localized increases in the magnitude of the data spread and abrupt changes in the value of the central tendency (e.g., $i = 60$ –70 “tea” data and $i = 70$ –80 “soda” data). It is thought that these instances are due to differences in student interpretation of when a bottle has fully emptied.

Another permutation of the single-bottle experiment is to provide students with the same type of bottle and to group the emptying time data that is collected. In this case, given the size of a class, a significant number of data points for a single bottle can be obtained in a short period of time. An example of the data that results is shown in Figure 5, where 75 students were provided with wine bottles of the same style and size. Each student was asked to contribute $n = 10$ values of bottle emptying time, yielding a total of $n = 750$. The data arranged in sequential order is provided in Figure 5a. Here, again we see the instances of abrupt changes in the magnitude of the central tendency for each student data cluster (e.g., $i = 200$ –210), which can be attributed to differences in student interpretation of the end of an emptying experiment. Given a large enough set of emptying times, the tendency is for the data to appear as though all values were collected from a single experimenter; this is especially true if the data is randomized. To see this, compare the sequential plots for the sequential and randomized data in Figure 5a. The histogram for this data is shown in Figure 5b where a subtle skewness is observed, when compared to the normal distribution, favoring a longer emptying time by a small fraction of students.

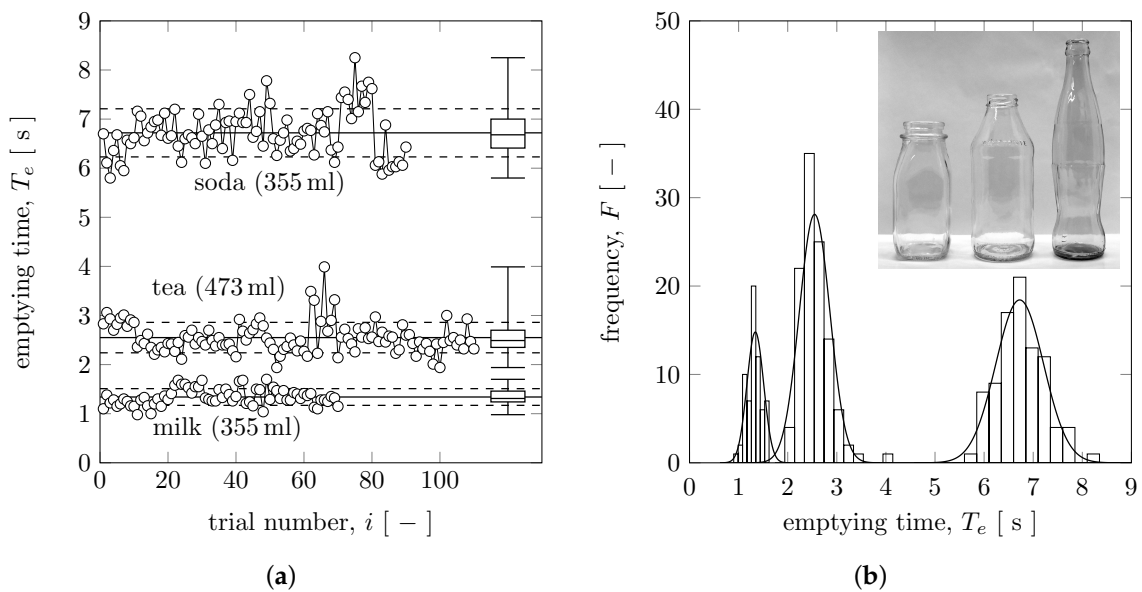


Figure 4. Emptying time data for several common bottles used by students. (a) Sequential plots and box-and-whisker plots suggest that emptying time is normally distributed, even when data is collected by many students instead of a single experimenter. Each student collected $n = 10$ values of emptying time. (b) Histograms and normal distributions also support the normalcy of the data. The inset shows the shape of the milk, tea, and soda bottles (arranged from left-to-right).

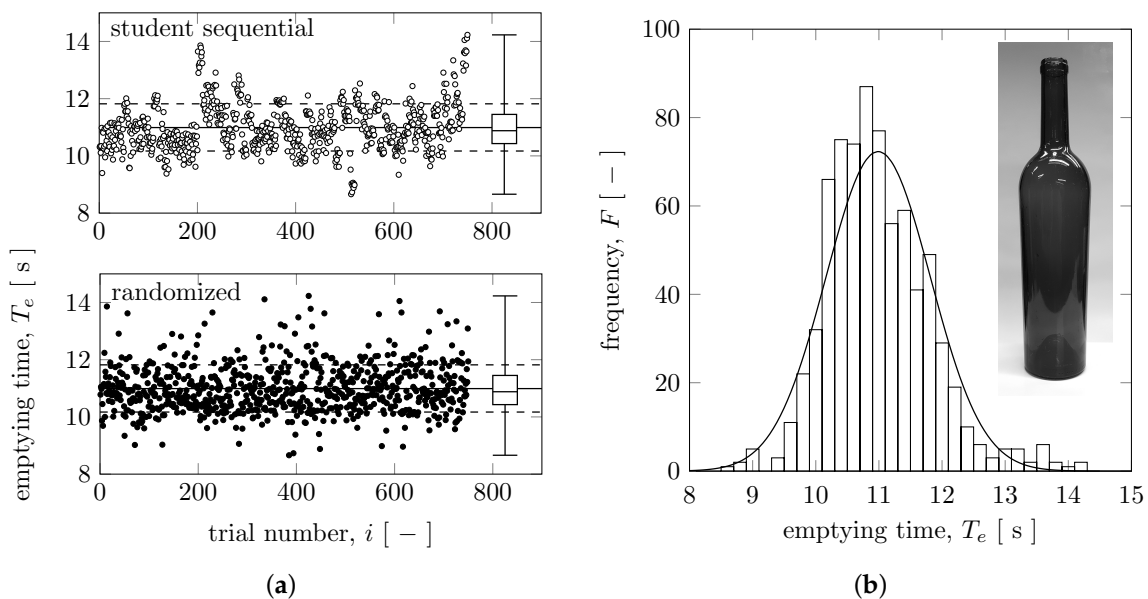


Figure 5. Emptying time data for wine bottles issued to 75 students. The unused wine bottles were procured in cases to ensure consistency in size and shape ($V = 750$ mL and $d = 18.4$ mm). (a) Sequential plots with box-and-whisker diagrams. The student sequential data (top, open circles) is ordered so that each group of 10 values belongs to a single student. When the sequential data is randomized (bottom, closed circles), it appears as though it were collected from a single individual. (b) The histogram suggests some skewness which is likely due to several students interpreting a longer emptying time.

2.3. Exercise 2—Interpreting the Body of Results (Multiple Bottles and Dimensional Analysis Focus)

2.3.1. Quantifying Experimental Uncertainty

Up to this point, we have considered the results from a few experiments performed using single bottles, and considered only statistical variations associated with the emptying time. However, there are other uncertainties in the measured quantities (e.g., emptying time, bottle volume, neck diameter, etc.)—we must at least account for the measurement uncertainties or resolution uncertainties connected to the bottle emptying experiments. Thus, before presenting the results from all student experiments, let us discuss the uncertainties associated with the individual measurements and combine those, when appropriate, with the statistical uncertainties developed in the previous section.

With regard to emptying time T_e , we have already considered the statistical uncertainty associated with multiple measurements; this is simply the confidence interval, $\pm t_{\nu} s / \sqrt{n}$. Recall that students were asked to perform $n = 3, 5, 10,$ or 25 trials and could use the results from these experiments to calculate the statistical uncertainty associated with the emptying time (using 95% confidence). There still exists the resolution uncertainty of the timers employed by the students. As these were typically cell phone app stopwatches, with stated resolutions of 0.01 or even 0.001 s, the resolution uncertainty, treated as one-half the instrument resolution [20], is negligible compared to the statistical uncertainty. However, due to manual timing of each trial, it would be more appropriate to consider errors due to human reaction time, as the dominant factor in the emptying time measurement error, not simply the resolution uncertainty. Although this can be the subject of further experimental study by students engaged in this exercise, a value of 0.25 s can be used to account for the total uncertainty in the reaction to the beginning and end of emptying (and, inherently, the perception of the emptying event, which is subject to interpretation). This value is typical of the range of human reaction time errors associated with stopwatch timing [22]. The reaction time was summed in quadrature with the timer resolution uncertainty and the statistical uncertainty to obtain an overall uncertainty in emptying time $u_{\bar{T}_e}$. The average value for this uncertainty for nearly all bottles tested was found to be 9.3%, although there are a number of instances (42 of 454 bottles) for which the uncertainty represents a significant fraction of the time, i.e., greater than 25%, due to fast emptying times (e.g., emptying times on the order of 1 s).

For bottle volume, students were provided access to either a graduated cylinder or a digital scale to make volumetric or gravimetric measurements. In general, using these techniques, the resolution uncertainty can be quite small. However, this can under predict the actual variation in filled volume that can occur during testing with the repeated inversion and waiting required by the procedure (which can lead to leaks). Because of this, it was decided to assign a reasonable uncertainty for bottle volume. Those bottles with $V \leq 50$ mL were assigned an uncertainty of 1 mL, whereas those with $V > 50$ mL were assigned an uncertainty of 5 mL. Many students reported using household measuring cups to determine volume, and the author even used bathroom and mechanical scales for certain large-volume bottles. Typically, these instances yielded values of uncertainty larger than those assigned. In all instances where the reported uncertainty exceeded the conservative values assigned based on volume, the larger uncertainty was used. For all of the bottles tested, the average uncertainty in bottle volume is 2.1%.

Similarly, the uncertainties in the measurements of neck diameter, u_d ; maximum diameter, u_D ; and height, u_h , were low (averages of 1.4%, 0.6%, and 0.4%, respectively), owing to the tools used by the students (e.g., ruler or caliper) in comparison to the size of the nominal values. All of the uncertainties discussed are summarized in Table 2 and are represented by error bars in the dimensional plots that follow. Having sorted out the uncertainties associated with the student measurements, we are now at a point where we can present the collection of bottle emptying data in dimensional form from all bottles, of various shapes and sizes, collected by students and the author.

Table 2. Measurement and statistical uncertainties for dimensional bottle emptying data.

Uncertainty	Average Value	Comment
u_V	2.1%	gravimetric/volumetric estimate
u_d	1.4%	measuring tool resolution uncertainty
u_D	0.6%	measuring tool resolution uncertainty
u_H	0.4%	measuring tool resolution uncertainty
$u_{\bar{T}_e}$	9.3%	overall uncertainty in \bar{T}_e

2.3.2. Bottle Emptying—Dimensional Results

From our most basic understanding of fluid mechanics, we expect that the emptying time for a bottle will increase with volume. This is essentially what is suggested by the data presented in Figure 6a, in which the average emptying time, \bar{T}_e , is plotted versus bottle volume, V . The error bars include measurement and statistical uncertainties as previously discussed. Despite our expectation regarding the relationship between emptying time and volume it is apparent that, without taking into account other geometric properties of the bottle, no useful predictive trend yielding a reasonably accurate estimate of emptying time can be extracted from such a dataset. There is simply too much scatter in the data as plotted. In fact there can exist more than an order of magnitude variation in emptying time for any fixed volume (e.g., see variation in \bar{T}_e for $V \sim 10^3$ mL). The lack of availability of very large commercially available bottles limits the data to the region $V \lesssim 3 \times 10^4$ mL.

Similarly, the lack of predictive power is also apparent in the plot of emptying time, \bar{T}_e , versus neck diameter, d , cf. Figure 6b. Again, our intuition leads us to believe that emptying time should decrease with increase in neck diameter; however, the overall picture in Figure 6b is not satisfactory for our purposes. Perhaps the only piece of information we can glean is that the majority of bottles have neck diameters in the neighborhood of $d \sim 20$ mm, which is not altogether surprising if we recognize that most of the bottles collected by students for these experiments are made for direct human consumption or convenient pouring. Finally, the remaining geometric measurements of maximum diameter, D , and height, H , are also not useful, by themselves, at establishing a predictive trend for emptying time, as shown in Figure 6c,d.

Recalling the motivation for this study, Figure 6 rules out the usefulness of the dimensional data to obtain a predictive relation for bottle emptying time (if one does exist). The figures clearly demonstrate that an assumption that the emptying time correlates with only one geometric variable is of no particular use. More than one dimension may be necessary. This conclusion leads us naturally to a discussion of dimensional analysis.

2.3.3. Dimensionless Groups Using Buckingham-Pi

Many undergraduate engineering students are first exposed to dimensional analysis in a fluid mechanics course, where the subdiscipline is considered in the context of experimental design and the arrangement of data to yield useful phenomenological relationships [23]. However, during this introduction, there is often a limited chance to see first-hand the power of dimensional analysis through application, i.e., the design of an experiment and the reduction of data. More often students complete typical textbook problems, the end result of which is the determination of dimensionless groups only. Without an applied experience, the main concepts and steps can be confusing, e.g., selection of repeating parameters in the use of the Buckingham-Pi theorem—a step described as requiring the “application of engineering judgment” and “experience” for a successful outcome [24], qualities that students are only beginning to develop.

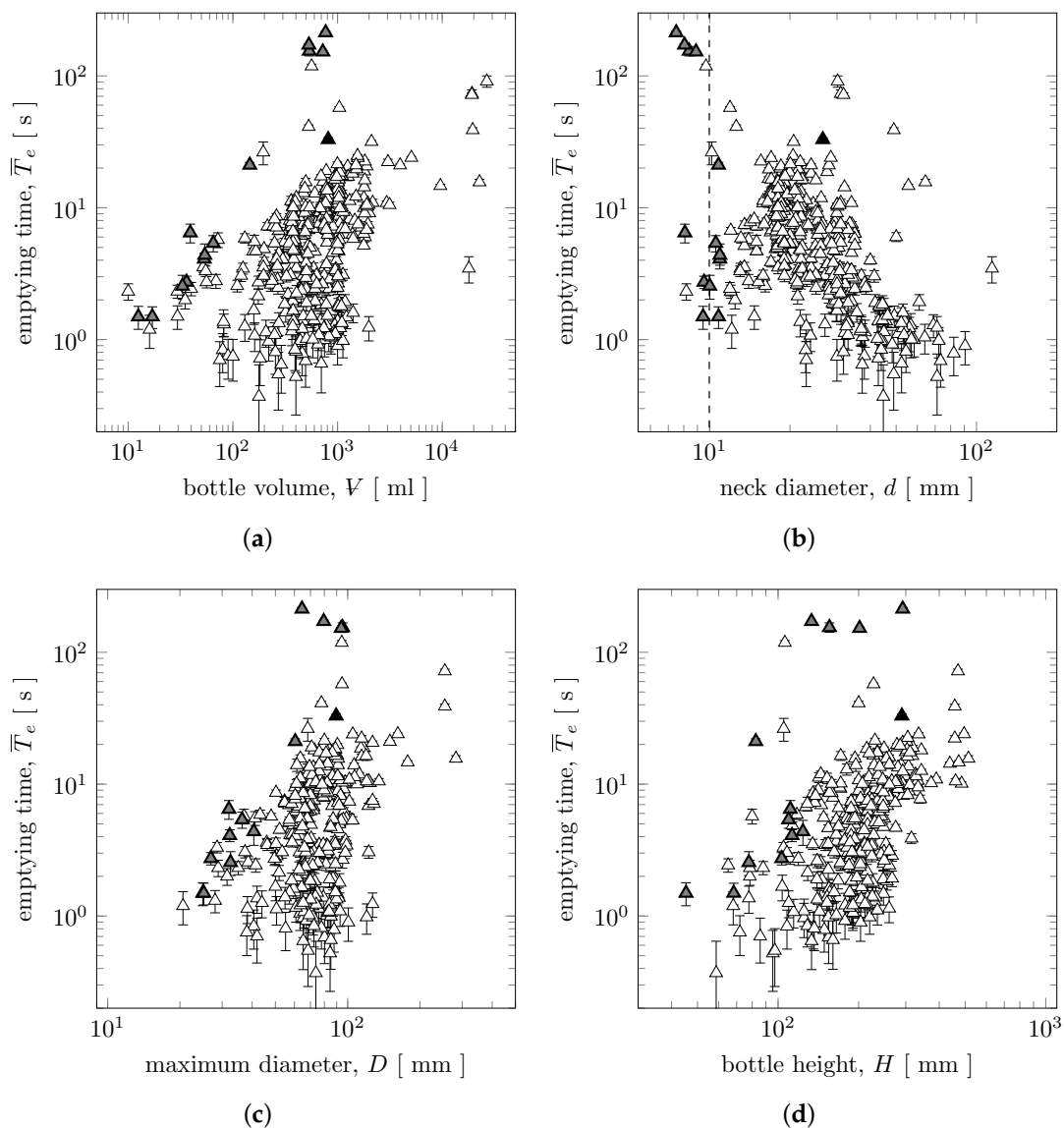


Figure 6. Emptying time versus the measured geometric dimensions for all bottles tested ($N = 454$). (a) Bottle emptying time generally increases with volume, but no predictive trend is apparent. The thirteen data points marked with gray triangles are the results from emptying small bottles with 70% isopropyl alcohol instead of water. The single black triangle denotes a data point for a bottle that has an internal decorative feature that can disrupt the flow. This was the only bottle tested with such a feature. (b) Neck diameter, d , alone is also not a good predictor of bottle emptying time; We observe that most bottles/containers collected by students tend to cluster around $d \sim 20$ mm, most likely a result of their intended use (liquids for direct consumption). It is also apparent that neck diameters are well in excess of the capillary length, $\sqrt{\gamma/(\rho g)} \sim 2.7$ mm. A number of small bottles tested by the author (gray triangles) have neck diameters less than the stable cut-off length associated with the Rayleigh–Taylor instability for a circular interface [25,26], i.e., $d_{RT} \sim 3.7\sqrt{\gamma/(\rho g)} \sim 10$ mm (dashed vertical line). For these cases, the emptying using water is essentially infinite, and so measurements have been made using 70% isopropyl alcohol to create the condition $d > d_{RT}$ by reducing the interfacial tension γ . This can be used to prompt added discussion among students during a presentation of the data. Note that three bottles with $d < d_{RT}$ were reported by students using water. It is suspected by the author that this was possible given nonideal neck conditions (e.g., a chip in one instance and a ground glass surface in another) or subtle off-vertical orientations that can readily occur during experiments; (c) maximum diameter D and (d) bottle height H do not, alone, provide a useful correlating variable for emptying time.

Given the lack of predictive trend apparent in the dimensional plots of Figure 6, the present goal is now to find relevant dimensionless groups that characterize the bottle emptying process—specifically the long timescale that characterizes complete emptying and not the short timescale associated with the familiar “glug-glug” [10], of which the latter phenomenon tends to dominate our casual observations. To be relevant for a discussion in an undergraduate fluid mechanics setting, the procedure for the Buckingham-Pi theorem as outlined in a typical fluid mechanics textbook is followed [24].

We can anticipate that for a liquid-filled bottle emptying into the atmosphere at room temperature and pressure, the emptying time T_e will be a function of many variables. For example, we might consider,

$$T_e = \phi_1(\rho, \mu, \gamma, g, H, D, d, S), \tag{1}$$

where ρ , μ , and γ are the relevant liquid properties (water density, viscosity, and liquid–air surface tension, respectively) and g is the gravitational acceleration. The geometry of the bottle is represented by an overall height and major diameter, H and D ; the neck diameter, d ; and a shape factor, which we designate S (cf. Figure 7). This term accounts for the complexity of the true bottle shape, including in particular the shape, length, and taper of the neck, and we will consider S as being dimensionless. In past studies on bottle emptying not involving the dimensional analysis approach taken here, the various shapes of the bottle used were presented diagrammatically with no effort made to quantify the details of the shape [3,4]. Or, conversely, specific experimental apparatuses were fabricated to provide well characterized containers for study. In the latter case, the exit condition (essentially an orifice plate, not a bottleneck) was described by a discharge coefficient [7]. Here, the sheer number of bottles ($N = 454$) prevents us from presenting a comprehensive diagram detailing each individual bottle shape (which can vary dramatically), and lack of control over shape by the use of commercially available bottles prohibits the specification of a known discharge coefficient and, therefore, the lumping of these qualities into S . Furthermore, given the myriad variations of real bottles and containers, we can expect that isolating separate trends based on characteristic bottle length and diameter will be too difficult for the present study. So, although we recognize it is a gross simplification, we will replace H and D with the total bottle volume V . This reduces the total number of variables in (1) from 9 to 8. The variables considered in (1) do not constitute an exhaustive list, and in the classroom setting it would be useful for an instructor to ask students to consider all other possible variables (including, but not limited to angle of inclination, amount of initial rotation/swirl, and surface roughness, all of which could be tested as additions to the work published in this study).

Continuing with the Buckingham-Pi methodology, after selecting three repeating parameters— ρ , g , and d —that characterize the fluid, flow field, and geometry for the emptying phenomenon (as well as capturing all primary dimensions in the set of variables), respectively, we see that there will be five dimensionless groups. Thus,

$$T_e \sqrt{\frac{g}{d}} = \phi_2 \left(\frac{\mu}{\rho \sqrt{gd^3}}, \frac{d}{\sqrt{\gamma/(\rho g)}}, \frac{V}{d^3}, S \right), \tag{2}$$

which do not present themselves as the typical dimensionless numbers encountered by undergraduates (e.g., Reynolds number, Re). Here, it should be mentioned that $\sqrt{\gamma/(\rho g)}$ is also referred to as the capillary length, l_c , and represents a length scale below which capillary forces (i.e., interfacial tension forces) become significant. For the present study, we are only interested in emptying bottles containing water into air at room temperature, and we will utilize bottles with neck diameters sufficient to rule out capillary effects (cf. Figure 6 caption). Therefore, the dimensionless group d/l_c will play no role. The inverse of the group $\mu/(\rho \sqrt{gd^3})$ is analogous to a Reynolds number (where \sqrt{gd} is a characteristic velocity). For all of the bottle emptying experiments, the value of $(\rho \sqrt{gd^3})/\mu$ exceeds 2000, and most (423 of 454) have values in excess of 5000. Thus, we can anticipate insignificant variations in experiments caused by this dimensionless parameter as nearly all flows will be turbulent. As a result, we neglect the independent dimensionless groups listed in (2) containing

the fluid properties. Further, neglecting for now the shape factor S (which we will return to later), the dimensional analysis suggests that we should present the data in the following form,

$$T_e \sqrt{\frac{g}{d}} = \phi_3 \left(\frac{V}{d^3} \right), \quad (3)$$

to look for a relationship between emptying time and bottle geometry. Whether or not we have picked the most relevant repeating parameters, or if we have over simplified our analysis, remains to be seen when we try to plot the data in dimensionless form.

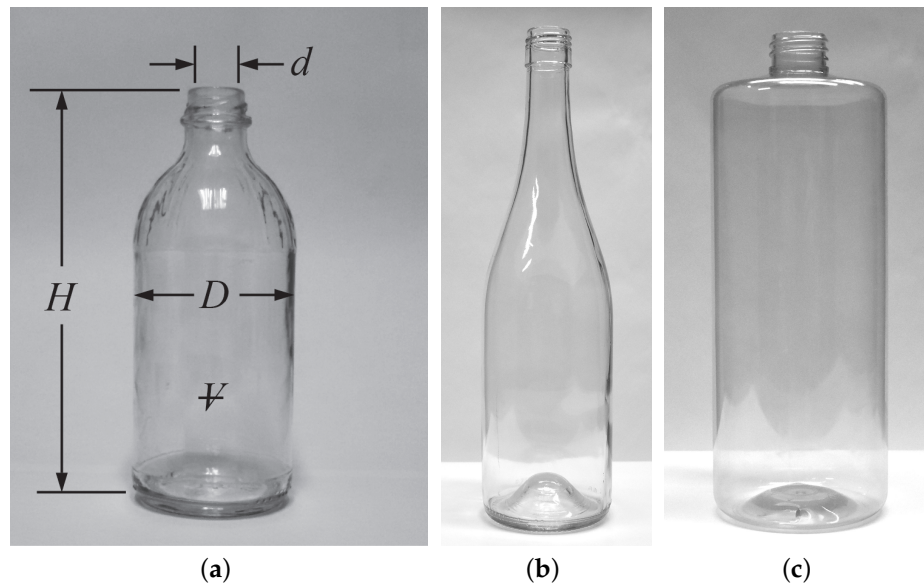


Figure 7. A visual description of bottle geometry relevant to the analysis of bottle emptying. (a) Dimensions associated with bottles used for emptying experiments: d , neck diameter (internal); D , major diameter; H , overall bottle height; and V , internal volume. It was used by the author for 100 measurements of emptying time (cf. Figure 2). (b) A bottleneck qualitatively classified as “smooth” due to the gradual evolution from D to d . This in sharp contrast to (c), which shows a bottleneck classified as “square”, as a result of the abrupt change from D to d . The bottle shown in (a) would be considered as something “other” than smooth or square.

2.3.4. Data Presented in Dimensionless Form

We can now plot the data in dimensionless form, and we do so according to the dimensionless groups presented in Equation (3). The result is shown in Figure 8. Error bars for dimensionless time and volume have been calculated by propagation of the uncertainties from each of the variables forming the dimensionless groups. Inspection of the figure shows it is clear that we arrived at relevant dimensionless groups in Section 2.3.3, based on the collapse of nearly all of the data points about, what appears to be, a single dominant trend—far different from the dimensional results in Figure 6. However, if we look at the data more closely, we can also see what looks like a difference in bottle emptying time based on the shape S . Earlier we had ignored the influence of the shape factor S , and the wide variety of shapes makes detailed classification based on such a factor difficult. However, for now, we can broadly classify the bottles as having a “smooth” neck (e.g., a wine bottle with a gradual taper from the average diameter to the neck), a “square” neck (i.e., minimal taper), or “other” if the bottle fails to be easily classified into the former groups. Examples of these classifications are shown in Figure 7, and we make no effort here to rigorously classify the shapes as it is beyond the scope of this work. The inset of Figure 8 indicates that many of the bottles with a more smooth neck appear to empty faster than square neck bottles of similar dimensionless volume. Further analysis of the data based

on a more rigorous classification of shape may provide a better prediction of bottle emptying time. Yet, for the purposes of this exercise, when the data is viewed as a whole it does suggest a general trend that is sufficient for engineering estimates of emptying time.

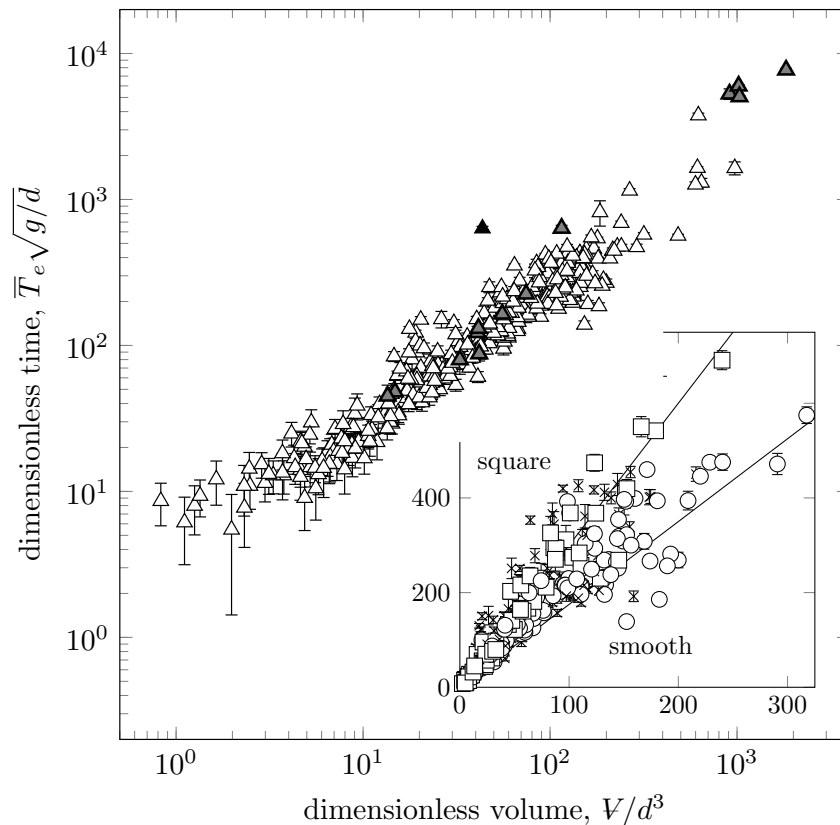


Figure 8. Data from bottle emptying experiments presented in dimensionless form according to the groups given in Equation (3). It is apparent that the data as a whole, despite variations in bottle shape and size, tend to collapse onto a single trend. However, greater scrutiny of the data, apparent in the inset (note the linear axes and reduced range and the symbol change—□ for square and ○ for smooth), shows what appears to be a difference in dimensionless emptying times based on bottle shape *S*. Smooth neck bottles empty faster than square necks. The solid lines in the inset are meant to guide the eye.

From the dimensionless data of Figure 8, it appears that a trend has emerged that allows us to make quantitative predictions for bottle emptying time as a function of volume and neck diameter. Our focus now shifts to determining an appropriate correlation using standard curve fitting techniques.

2.4. Exercise 3—Developing an Empirical Correlation (Regression Analysis)

The goal of the analysis in this section is to obtain a curve fit for the data presented in Figure 8, i.e., to elucidate the relationship between $\bar{T}_e \sqrt{g/d}$ and V/d^3 , so that we can determine with sufficient accuracy the emptying time for any future bottle or single outlet container. A curve fit for the data will be determined using a method of least-squares analysis and we have provided details and equations in Appendix C.

2.4.1. Regression Analysis

In general, we can utilize the known physics of a phenomenon to guide the appropriate choice of a model for curve fitting of data. However, in the case of bottle emptying, where the fluid dynamics appear complex, we are left to wonder what is the appropriate choice for a curve fit. The method

of least-squares, which is what we will eventually use, can only be applied after the order of the polynomial curve fit has been decided, and it is unacceptable to arbitrarily choose the order. What then are we left with? In this instance, let us consider the span of the data for both coordinates.

For both $\bar{T}_e\sqrt{g/d}$ and Ψ/d^3 , the data extends over several orders of magnitude, so a log–log format is the best choice for plotting the data. Inspection of the data, as shown in Figure 8, plotted on the log–log axis and appearing linear suggests that indeed a power–law curve fit between the dimensionless groups may be appropriate [20]. Thus, regression analysis will be used to find the best-fit coefficient A and the exponent B for a power–law function of the form $\bar{T}_e\sqrt{g/d} = A (\Psi/d^3)^B$. Only the data for small values of dimensionless volume, i.e., $\Psi/d^3 \lesssim 3$ hint at a deviation from linearity. This change in behavior is likely based on a change in the fundamental shape of the bottles at these scales. For these values of Ψ/d^3 the bottles are really jars, mugs, or cups, instead of a bottle with what we think of as a neck, e.g., with $d < D$. These vessels, when emptying, do not “glug”. Rather, drainage proceeds as a single bubble of air rises into vessel along one side and liquid drops from the other. This is also in contrast to the emptying of a long narrow tube [1,2].

The power–law curve fit can be obtained using a method of least-squares approach for a linear regression, e.g., $y = a_0 + a_1x$, after a standard linear transformation has been performed. In other words, to make use of the equations for the regression coefficients a_0 and a_1 in the standard first-order curve fit (familiar to most students in a first course on statistics), we must first transform our variables such that $\bar{T}_e\sqrt{g/d} \rightarrow y$ and $\Psi/d^3 \rightarrow x$. For a power law, this is accomplished using natural logarithms. Thus,

$$\bar{T}_e\sqrt{g/d} = A (\Psi/d^3)^B \rightarrow y = a_0 + a_1x \tag{4}$$

with $y = \ln[\bar{T}_e\sqrt{g/d}]$, $x = \ln[\Psi/d^3]$, and $a_0 = \ln A$ and $a_1 = B$. What remains is to solve for the regression coefficients [16] a_0 (Equation (A10)) and a_1 (Equation (A11)), and then transform back to find A and B . This analysis yields the following power–law curve fit to all of the data,

$$\bar{T}_e\sqrt{\frac{g}{d}} = (3.8 \pm 0.4) \left(\frac{\Psi}{d^3}\right)^{(0.90 \pm 0.02)}, \tag{5}$$

which is plotted in Figure 9a, along with uncertainty bands (based on 95% confidence) qualitatively demonstrating how well the regression equation (solid line) predicts the mean of the data (inner set of dashed lines) and the uncertainty that the regression equation can predict any single value (outer dashed line). Not surprisingly, given the appearance of the dimensionless data in Figure 8, the power law correlation fits the data over the nearly four orders of magnitude spanned by Ψ/d^3 .

The variation of individual data points about the curve fit line is presented in Figure 9b. Here, the variation is expressed as a normalized residual r , defined as the difference between the experimental and curve fit values of $\bar{T}_e\sqrt{g/d}$, normalized by the curve fit value. The purpose of normalizing the residuals is to account for the difference between experimental values, and curve fit values inherently increasing in magnitude with increase in dimensionless volume. What we find from a review of these figures is that the normalized residuals are scattered somewhat symmetrically about zero, without any apparent trend that would indicate a more appropriate curve fit model exists. More specifically, the values of r appear to be distributed normally about zero when a histogram is generated over the entire range of Ψ/d^3 . The average value is calculated to be $r = 5\%$ with an average absolute value of $|r| = 25\%$.

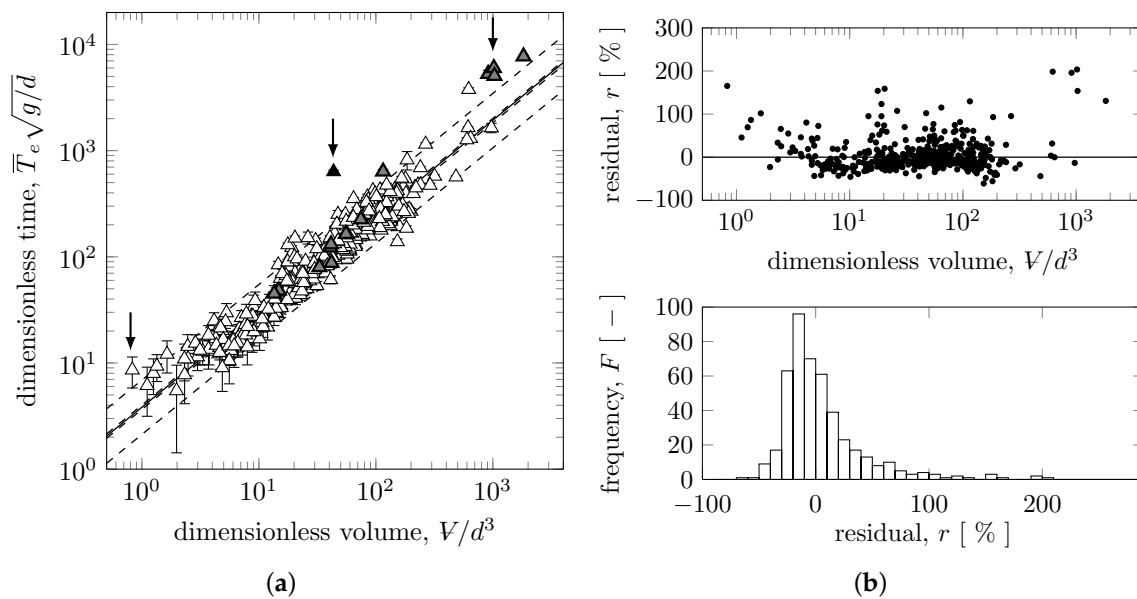


Figure 9. (a) Data from bottle emptying experiments presented in dimensionless form according to the groups given in Equation (3) along with the power-law curve fit of Equation (5) (solid line). Added to these plots are confidence intervals for the curve fit (95% confidence). The inner set of dashed lines, almost indistinguishable from the solid line, indicates the confidence that the curve fit can estimate the mean value of the population, whereas the outer set of dashed lines denotes the confidence that the curve fit can predict any individual value of the ordinate. Arrows highlight bottles that deviate significantly from the power-law fit. The bottle with the internal feature (black triangle) was not used in the curve fit analysis but is shown to indicate the effect of the internal feature on the emptying time. (b) Discrepancy between experimental data and power-law curve fit (Equation (5)) expressed as a normalized residual, r (% units). (Top) The scatter of r about zero for the entire range of the dimensionless volume shows no apparent trend, but a few data points show considerable deviation from the curve fit (i.e., r exceeds 100%). (Bottom) Values of r appear to be symmetrically, almost normally, distributed about a value near zero.

2.4.2. Trend Deviations

The data points with the most significant values of r , e.g., $\sim 200\%$, are at the extreme ends of the V/d^3 range. These are highlighted by the arrows in Figure 9a at $V/d^3 \sim 1$ and $V/d^3 \sim 10^3$. Note that these single-outlet vessels are the furthest, in shape/style, from what we might think of as a typical “bottle”. As shown in Figure 10a, the data point at $V/d^3 \sim 1$ corresponds to a pint glass, where $d \approx D$ without a true neck. The data points clustered near $V/d^3 \sim 10^3$ are for reusable tumblers with a thin lid and rounded orifice intended for a straw (cf. Figure 10b). Although for this container $d \ll D$, the shape is still far from a traditional bottle since, like a pint glass, there is also no true neck.

Every bottle in the dataset ($N = 454$) used to generate Equation (5) shared the characteristic that the internal space of the vessel was empty and that there were no obstructions within the neck. A single bottle provided by a student, highlighted by the arrow in Figure 9a at $V/d^3 \sim 40$, contained an internal decorative feature as well as a bridge of glass material that spanned the neck at its base. Both of these features can be seen in Figure 10c. Because of these features, the data collected from experiments in this bottle was not used in the analysis to obtain a curve fit (and does not constitute one of the $N = 454$ data points). However, it has been included in nearly all of the dimensional and dimensionless plots, with the exception of Figure 9b, to show the effects of the features on the emptying time. A comparison of the dimensionless emptying time for this bottle to that predicted by Equation (5) yields a value of $r = 450\%$. Looking back at the sequence of images in Figure 1, it is easy to imagine how disruptive the internal decorative feature would be on the inflow of air and

outflow of water near the bottleneck. In addition, it is estimated that the bridge of glass within the neck reduces the flow passage area by nearly $1/3$ – $1/2$ the area calculated using the neck diameter. Both explanations are likely responsible for causing the large value of r for this particular bottle. The neck diameter for this bottle was measured as $d = 26.55$ mm, along with a volume of $V = 814$ mL, giving the value of $V/d^3 \sim 40$ reported. If we estimate that the flow passage area of the neck is restricted by $1/3$, we arrive at an equivalent neck diameter of $d = 21.7$ mm, a value of $V/d^3 \sim 80$, and $r = 218\%$. With a flow passage area restricted by $1/2$, an equivalent neck diameter of $d = 18.8$ mm results, yielding $V/d^3 \sim 120$ and $r = 118\%$. Although these are estimates, we can anticipate that with $r \gtrsim 120\%$, the discrepancy is due not only to the obstruction of the neck but the internal decorative feature as well.



Figure 10. Images of three “bottles” that yield significant values of r when compared to the power-law curve fit of the dimensionless data (indicated with arrows in Figure 9a). (a) Typical pint glass with $V/d^3 \sim 1$. (b) Reusable plastic tumbler ($V/d^3 \sim 10^3$) with a small hole in the lid intended for a straw. (c) A bottle with an large and obstructive internal decorative feature (left) along with a glass bridge across the flow passage at the base of the neck (right—imaged from side of bottle looking up at the base of the neck).

2.5. Exercise 4—Comparison of Empirical Correlation to Available Results

2.5.1. A Substantial Data Set

We now depart from the statistics and dimensional analysis content for a review of the sparse datasets and simple analytical models available in the literature, which we will compare to our experimental findings presented in Figures 8 and 9. This section, although not necessary for an exercise in either engineering statistics or dimensional analysis, does provide some physical insight into the emptying of a single-outlet vessel and reinforces the selection of a power-law curve fit to best describe the data. The choice to present this content to the student group or to let them research on their own would depend on the academic level of the fluid mechanics course. Note, here, the dramatic difference between datasets in the literature and the substantial set of new data in the present work. Figure 11a shows this difference. Here, we can see the range of both V and d spanned by the $N = 454$ bottles from the present work, as compared to the data extracted from the works of Whalley [3,4] (16 bottles), Tehrani et al. [6] (four bottles), and Geiger et al. [11] (two bottles simulated using CFD).

2.5.2. Published Results and Models

Whalley [3,4] investigated the emptying time of bottles via simple experiments and related the outflow to the phenomenon of “flooding” in tubes—a well-researched subject in the field of multiphase flows. He presented his experimental results in dimensional form (i.e., emptying time) and also calculated a Wallis flooding “constant”, C , using

$$C = \frac{(\rho_G^{1/4} + \rho_L^{1/4})}{[(\rho_L - \rho_G)gd]^{1/4}} \left(\frac{4V}{\pi d^2 T_e} \right)^{1/2}, \tag{6}$$

where ρ_G and ρ_L are the densities of air and water, respectively. This semiempirical relationship has its basis in a correlation for flooding that utilizes dimensionless superficial gas and liquid velocities, and is consistent with the simple picture that during the entire course of emptying, a stationary air slug exists in the bottleneck with a continuous outflow of water around the slug [3,4] (i.e., slugging). The velocity of liquid outflow is equivalent, by continuity, to the rising velocity of the gas slug (as given by Davies and Taylor [1]). To visualize this, consider the fourth image in Figure 1a with the slug in the bottleneck and envision that this picture of the flow persists over the entire course of emptying as hinted at by the overlay of images shown in Figure 1b. Both sets of data from Whalley’s experiments, specifically the 11-bottle set from his earlier work [3] and the 5-bottle set from his later work [4], show a range of calculated values for C from 0.76 to 1.02 with an average value of $\bar{C} = 0.91$. Kordestani and Kubie [8], who also expressed their results for ideal bottles in terms of C , found a similar range of values spanning approximately 0.8 to 1.15. Using the values for ρ_G and ρ_L of air and water at room temperature, the average value of C from Whalley’s works, and rearranging Equation (6) to reflect the dimensionless groups obtained from our analysis in Section 2.3.3, reveals the following,

$$T_{e,W} \sqrt{\frac{g}{d}} = 2.2 \left(\frac{V}{d^3} \right)^1. \tag{7}$$

The W subscript in $T_{e,W}$ is intended to distinguish this Whalley result from others. Given the variation in values of C , the coefficient in Equation (7) has a range of 1.7 to 3.1 with the exponent of V/d^3 unaffected by changes in C . Although the coefficient differs by a little less than a factor of 2 from that of Equation (5), the overall trend is similar to that exhibited by our data as demonstrated by the dashed line in Figure 11b (Equation (7) plotted). Quantitative comparison of our data with the result of Whalley, using our previously defined normalized variable, yields $r = 30\%$ and $|\bar{r}| = 36\%$. We can also see in Figure 11b how well our data overlaps and extends the limited set of data from Whalley [3,4].

Clanet & Searby [10] analyzed the emptying of “ideal” vertically-oriented bottles (i.e., bottles with constant diameter and very short sharp-edged openings manufactured specifically for laboratory experiments). Their model of the long timescale, the overall emptying time T_e —not the timescale associated with passage of individual slugs of air through the opening, is based on similar physics to that of Whalley, but not described from the standpoint of accepted two-phase flow correlations. Rather, these authors build their simple model from the required balance between the incoming air at the opening and the downward motion of the air–water interface in the bottle. They use the rise speed of a long bubble in an infinite medium (again, from Davies and Taylor [1]) to characterize the incoming airflow, and make the assumption that the length of the incoming bubble is equivalent to the opening diameter (recall that their “ideal” bottles have no true neck length—therefore the diameter of the opening serves as a relevant scale for the length of the incoming bubbles). Clanet & Searby present their model for the long timescale as $T_e/T_{e,0} = (D/d)^{5/2}$. In their model, $T_{e,0} \simeq 3.0L/\sqrt{gD}$ is the emptying time of an unrestricted cylinder of length L and diameter D . This model yields the following estimate for the emptying time (using $V = (\pi/4)D^2L$ and after rearrangement to be consistent with present form),

$$T_{e,CS} \sqrt{\frac{g}{d}} = 3.8 \left(\frac{V}{d^3} \right)^1. \tag{8}$$

We also plotted this trend in Figure 11b for visual comparison, and, quantitatively, we find that $r = -26\%$ and $|\bar{r}| = 34\%$. Equation (8) has the same scaling for V/d^3 as the result of Whalley, and is similar to the results of the present study, although there is incomplete agreement with the power-law

exponent. The exponent associated with V/d^3 from both Whalley and Clanet & Searby does not fall within the error of the experimentally determined exponent in the present work and differs by 10%.

The remaining data found in the literature that pertain to emptying of real bottles is found in the CFD analysis of Geiger et al. [11] and the experiments of Tehrani et al. [6], and this too is found to compare favorably with the new data presented here. A final inspection of Figure 11b shows that nearly all of the plotted data points tend to fall between the predictions of Whalley and Clanet & Searby, and that the power-law fit to our experimental data spans the two models over the range investigated.

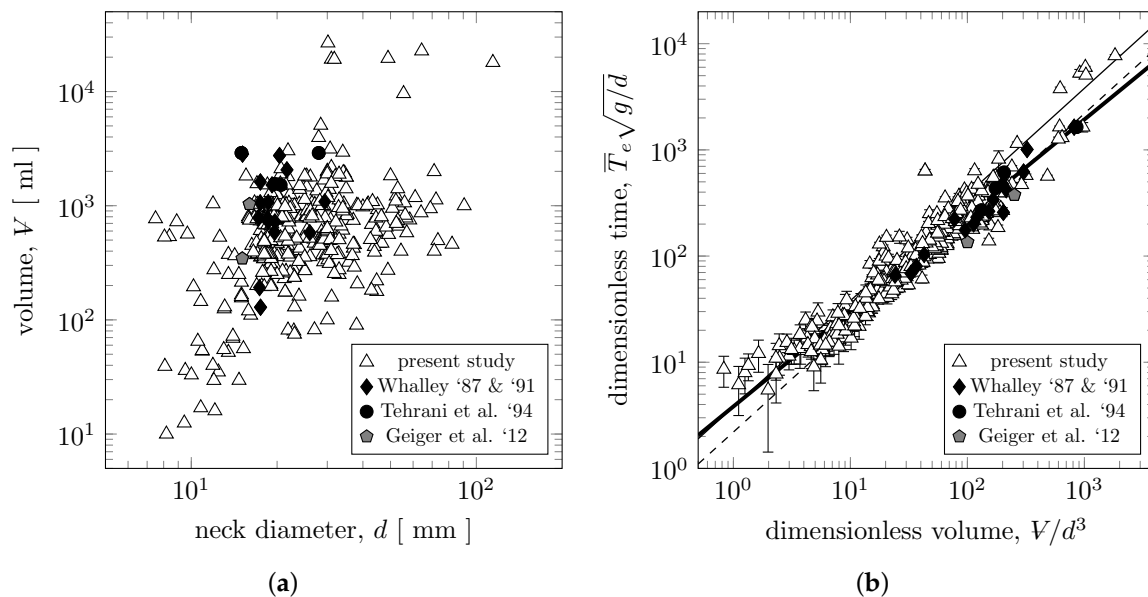


Figure 11. (a) Dimensions of the bottles from experiments of students (present work) plotted with limited datasets found in the literature, specifically those of Whalley [3,4], Tehrani et al. [6], and Geiger et al. [11]. The dataset collected by students is nearly twenty times larger than the collective data of the literature and contains bottles that span approximately 0.25–10× the volumes previously tested. The range of bottle diameters tested are also much larger, and smaller, than those previously explored. (b) Data from bottle emptying experiments of students plotted with limited datasets found in the literature, specifically those of Whalley [3,4], Tehrani et al. [6], and Geiger et al. [11]. The trend line from our data, Equation (5), is shown (thick solid line), as is the model of Clanet and Searby, Equation (8) (thin solid line) and that of Whalley, Equation (7) (dashed line).

2.5.3. Revisiting Regression Analysis

As a final note, given the exponent associated with V/d^3 in the models of Whalley and Clanet and Searby, perhaps it is worth revisiting our regression analysis, now that we have some knowledge of the physics at hand (recall from Section 2.4.1 that we typically rely on the physics to guide our choice of curve fit function). What the models of Whalley and Clanet and Searby suggest is that we could also seek a curve fit of the form $\bar{T}_e \sqrt{g/d} = A (V/d^3)^1$, where the exponent has been set to 1. This is analogous to finding a linear curve fit with zero intercept, i.e., $y = a_1 * x$ (note that this is not the same a_1 as defined by Equation (A11); therefore, we must use Equation (A12)). If we perform such an analysis, we arrive at the following fit to our data,

$$\bar{T}_e \sqrt{\frac{g}{d}} = (3.7 \pm 0.2) \left(\frac{V}{d^3} \right)^1. \tag{9}$$

This is nearly identical and, given the uncertainty range, it is equivalent to the model of Clanet and Searby (Equation (8)). The nominal value of the coefficient differs by nearly a factor of two compared

to the equation of Whalley (Equation (7)). A summary of all of the empirical models and analytical models from the literature is provided in Table 3.

Table 3. Summary of the regression models developed in this work and the simple analytical models obtained from the literature. All models have the form of a power-law function, with A as the coefficient and B the exponent.

Source	Equation	Coefficient A	Exponent B
present work	(5)	3.8 ± 0.4	0.90 ± 0.02
present work	(9)	3.7 ± 0.2	1
Whalley [3,4]	(7)	2.2 (1.7 – 3.1)	1
Clanet & Searby [10]	(8)	3.8	1

2.6. Very Large Bottles—Does the Trend End?

A goal of the present study was to experiment with only commercially and readily available bottles so that no special equipment or experimental apparatus is necessary (an example of this equipment would be the “ideal” bottles used in the literature). This goal was achieved, and any class that is asked to perform this exercise will likely find a similar range of bottle shapes and sizes yielding consistent results. Ignoring the data corresponding to very small values of \mathcal{V}/d^3 , the trend in the dimensionless data of Figure 8 appears to hold for the entire range of \mathcal{V}/d^3 , and it has always piqued the interest of the author to ask if there is an upper limit to the applicability of this trend. However, addressing this question requires going beyond commercially available bottles, and building bottles to suit the needs of the experiment. There are only two ways to achieve ever larger values of \mathcal{V}/d^3 : (1) reduce the neck diameter d of a bottle and (2) increase the volume \mathcal{V} of a bottle. As we have seen, there is a limit to the reduction in the neck diameter governed by capillary effects and the Rayleigh–Taylor instability, which will prevent emptying. Therefore, the only practical way of achieving very large values of \mathcal{V}/d^3 is to use large volumes.

To explore bottle emptying for large values of \mathcal{V}/d^3 , i.e., $\mathcal{V}/d^3 \gtrsim 5 \times 10^3$ (which is approximately the limit for the commercially available bottles found by students and the author), the author resorted to the fabrication of bottles using both a 15-gallon and a 55 gallon plastic drum (these are nominal volumes—the measured volumes were found to be 64,500 mL and 225,000 mL representing an increase in volume of $2.4 \times 8.3 \times$ compared to the largest bottle in the $N = 454$ set). These drums, shown in Figure 12a, were outfitted with interchangeable 3D printed necks with measurements of $d = 12.5, 25,$ and 37.5 mm. The necks were fitted to the drums using machine screws and sealed with gaskets. These inverted bottles were secured in a vertical orientation on an elevated stand. Garbage cans directly below the bottles were used to collect and recycle the water during the experiments. Each bottle was filled by means of a centrifugal pump using the bung hole (which was sealed with the threaded and gasketed bung).

The emptying times for these bottles ranged from approximately 110–1500 s (15 gallons) to 400–6100 s (55 gallons), with the emptying time decreasing with increasing d . The combination of bottle volume and neck diameters result in values of \mathcal{V}/d^3 spanning from nearly 10^3 to 10^5 —almost two orders of magnitude larger than the commercially available bottle set. Despite the dramatic increase in dimensionless bottle volume, and to the delight of the student audience that this is presented to, the trend persists and the agreement between Equation (5) is qualitatively on display in Figure 12b. Quantitatively, for the 15-gallon bottles, $|\overline{r}| = 17\%$, and for the 55-gallon bottles, $|\overline{r}| = 21\%$. Both values of $|\overline{r}|$ are within the value of 25 % reported earlier for the $N = 454$ dataset. It is left to another group of experimentalists, perhaps a motivated student group, to continue to push the limits of \mathcal{V}/d^3 .

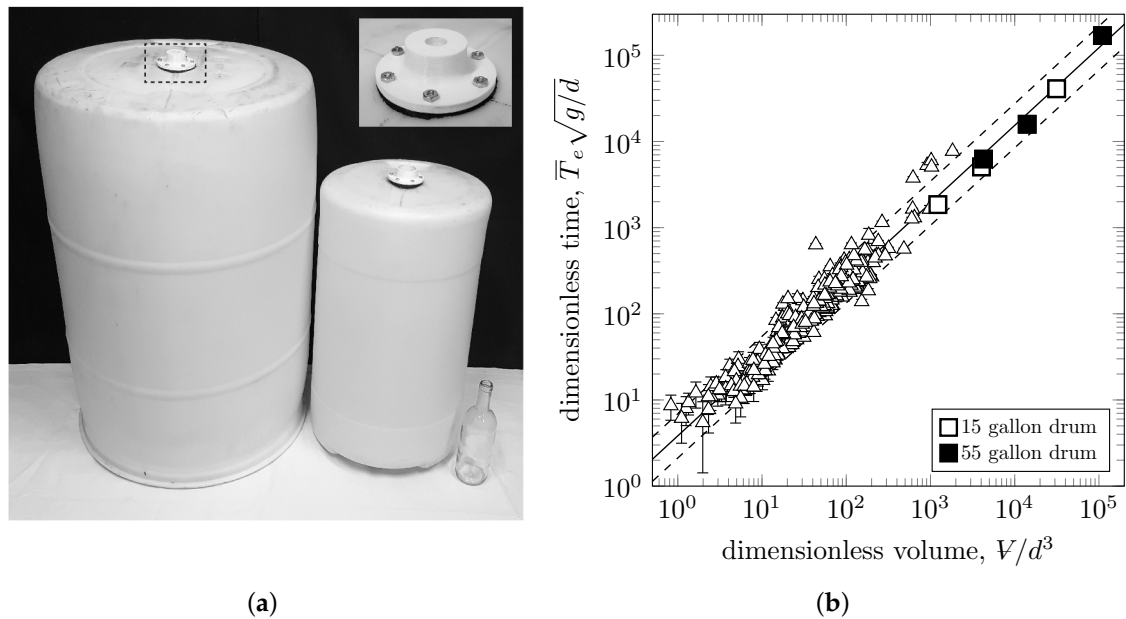


Figure 12. Very large bottles that can significantly extend the values of V/d^3 from the $N = 454$ dataset are not readily available. (a) The author resorted to manufacturing bottles using commercially available plastic drums (15-gallon and 55-gallon) and 3D printed necks (see inset image) to achieve over an order of magnitude increase in V/d^3 . A wine bottle is shown in the image for scale. (b) The results of these large bottle emptying experiments are consistent with the data and curve fit presented.

3. Conclusions

We have presented an exercise suitable for an undergraduate engineering statistics class, as well as a course in which the basics of dimensional analysis are presented—the ideal venue being an introductory fluid mechanics course. The exercise involves a large dataset that can be gathered safely and easily by students, without resorting to expensive laboratory equipment or complex procedures. Basic descriptive and inferential statistics are suitable to describe the data. The every day phenomenon under investigation is rather complex and, to an undergraduate student first encountering fluid mechanics, it may not appear to be accessible by normal analytic means. Results presented here clearly demonstrate the power of dimensional analysis in reducing the data to yield a predictive trend and the results agree well with the limited set of data available and simple models developed in the literature. The variations of this particular exercise are myriad, and many of the experiments could still be performed with basic equipment. For example, an instructor could task the students with confirming the variation in emptying time with water temperature [3,4,6], or variations associated with inclination [3,4,9]. Students could be directed to establish the relevance of another dimensionless group by experimenting with differences in liquid viscosity (or ratios of density or viscosity). Filling time, rather than emptying time, could also be explored. Greater detail as to the role shape plays can be elucidated, and, given the appearance of g within the dimensionless emptying time, perhaps bottles could be emptied with the aid of centrifugal forces. There is no doubt that students could be tasked with, and would be eager about, finding a modification to this exercise that is worthy of study. These and other variations can be accomplished in the spirit of the work presented here and we encourage others to explore similar activities for the benefit of engineering students at their respective universities.

Supplementary Materials: The following are available online at www.mdpi.com/xxx/s1.

Author Contributions: H.C.M. is responsible for all aspects of this article except for portions of the raw data contributed by students.

Funding: This research received no external funding.

Acknowledgments: The author would like to thank the numerous students at Cal Poly SLO, UCSB, and Rutgers University from 2007 to 2019 who helped gather data during their undergraduate statistics/measurements and fluid mechanics courses. Without their help over the last decade, the dataset would not have been as large or as interesting. The author would also like to acknowledge Professors G. Thorncroft, P. Lemieux, J. Maddren (Cal Poly SLO), S. Pennathur (UCSB), R. Krechetnikov (U. Alberta), and S. Shojaei-Zadeh (Rutgers) for providing useful feedback on earlier drafts of the manuscripts.

Conflicts of Interest: The author declares no conflict of interest.

Appendix A. Descriptive Statistics

Equations for the basic statistics used throughout the paper are presented here for the interested reader. In what follows in this section, emphasizing descriptive statistics, we will use the typical variable notation x to denote our measured quantity under investigation (whereas in the body of the paper we used T_e).

The most commonly used measure of the central tendency is the arithmetic mean (i.e., the mean) and is defined as

$$\bar{x} = \frac{1}{n} \sum_{i=1}^n x_i, \quad (\text{A1})$$

where n is the size of the sample and i denotes the number in the sequential dataset.

The sample standard deviation s is a single measure characterizing the spread of the data about the central tendency. For a sample of size n , it can be calculated using

$$s = \sqrt{\frac{1}{n-1} \sum_{i=1}^n (x_i - \bar{x})^2}. \quad (\text{A2})$$

The standard deviation can be considered as a kind of “average” distance the data sits, as a whole, from the central tendency.

Although we can visualize the shape of the data by developing a frequency distribution, we can also quantify the symmetry and peakedness of the distribution by calculating the skewness Sk and kurtosis Ku , respectively. We use the following definitions for calculations of each measure,

$$Sk = \frac{1}{(n-1)s^3} \sum_{i=1}^n (x_i - \bar{x})^3, \quad (\text{A3})$$

and

$$Ku = \frac{1}{(n-1)s^4} \sum_{i=1}^n (x_i - \bar{x})^4. \quad (\text{A4})$$

Appendix B. The Student- T and Gaussian (Normal) Distributions

Here, we present equations related to inferential statistics and standard distributions used throughout the paper, in particular to estimate the statistical uncertainty associated with multiple measurements of bottle emptying time. Again, we use x in lieu of T_e .

For a sample (implying finite size) of x_i of size n whose parent population is normally distributed, we can estimate the population mean μ using the Student’s t variable. This estimate is given as

$$\mu = \bar{x} \pm \frac{t_v s}{\sqrt{n}}, \quad (\text{A5})$$

where t_v is tabulated for various levels of confidence. Often the term $\pm(t_v s)/\sqrt{n}$ is referred to as the “confidence interval”.

The probability density function for a normally distributed variable,

$$p(x) = \frac{1}{\sigma\sqrt{2\pi}} e^{-(x-\mu)^2/2\sigma^2}. \quad (\text{A6})$$

is familiar to many students in science and engineering disciplines. As a refresher, the probability density $p(x)$ is related to the probability that x will lie between values a and b , i.e., $P(a < x < b)$ via

$$P(a < x < b) = \int_a^b p(x)dx. \tag{A7}$$

Additionally, for small values of Δx , we can write that $P(x < X < x + \Delta x) = p(x)\Delta x$. We are interested in relating this back to the finite data that we have to work with, specifically so as to visually compare to the frequency distribution in Figure 2b. Thus, we must use $P = F/n$, which then allows us to write that $F(x) = np(x)\Delta x$. Using this finding and Equation (A6) we can create a continuous curve $F(x)$ that can be superimposed onto a frequency distribution, i.e.,

$$F(x) = n \left(\frac{1}{\sigma\sqrt{2\pi}} e^{-(x-\mu)^2/2\sigma^2} \right) \Delta x. \tag{A8}$$

Alternatively we can transform the frequency data for x into the corresponding probability density. The probability density for each bin, l , in the frequency distribution (where $l = 1\dots k$) can be calculated using our definition of the probability density $p_l = f_l/\Delta x$, where $f_l = F_l/n$ is the relative frequency. One advantage to this approach is that bar charts of probability density, rather than frequency F , demonstrate that probability density values are nearly independent of bin width and will approach limiting values i.e., a limiting distribution, as $n \rightarrow \infty$ and $\Delta x \rightarrow 0$.

To quantitatively assess whether a normal distribution adequately fits the data, we used the Kolmogorov–Smirnov test [27]. In this test, we first compute the maximum of the deviation, d_{KS} , between the empirical cumulative relative frequency, cf , to theoretical value from a standard distribution. For our case this is the normal distribution, but this test is not restricted to this distribution only. The maximum of the deviation just described can be expressed as

$$d_{KS} = \max_{1 \leq j \leq n} |cf(x_j) - cf_n(x_j)|, \tag{A9}$$

where $cf(x_j)$ is the cumulative relative frequency (i.e., bounded by 0 and 1) based on the theoretical distribution for a population, and $cf_n(x_j) = j/n$ is the empirical cumulative relative frequency. Here, the index j denotes the ordered dataset. We then compare the value of the maximum deviation d_{KS} to the critical value $d_\alpha(n)$ based on the sample size, n , and the level of significance α (critical values are tabulated [27]). If $d_{KS} < d_\alpha(n)$, the theoretical distribution passes the test. If $d_{KS} > d_\alpha(n)$, the discrepancy between the empirical cumulative frequency distribution and the theoretical distribution is considered significant and the theoretical distribution fails to represent the data.

Appendix C. Regression Analysis

For the necessary material related to regression analysis, which is needed to find the empirical correlation describing the entire set of our bottle emptying data, we transition from the statistics of a single variable x to the relationship between two variables $y(x)$. In what follows, the notion that we use here now reflects $x \rightarrow V/d^3$ and $y \rightarrow \bar{T}_e \sqrt{g/d}$.

The method of least squares can be used to find the best-fit polynomial function of the form $y = a_0 + a_1x + a_2x^2 + \dots + a_mx^m$ through a set of n data points (x_i, y_i) once the order of the polynomial, m , has been selected. For a linear regression of the form $y = a_0 + a_1x$, the method is straightforward and reduces to solving for the regression coefficients [16] a_0 and a_1 , which minimizes the deviation between the curve fit equation and the data points. Here, we provide the definitions for a_0 and a_1 :

$$a_0 = \frac{\sum x_i \sum x_i y_i - \sum x_i^2 \sum y_i}{(\sum x_i)^2 - n \sum x_i^2} \quad \text{and} \tag{A10}$$

$$a_1 = \frac{\sum x_i \sum y_i - n \sum x_i y_i}{(\sum x_i)^2 - n \sum x_i^2}. \quad (\text{A11})$$

The summation symbols have been simplified but all apply from $i = 1 \dots n$. Although a program (e.g., Excel[®] or MATLAB[®]) can be used to automatically solve for these coefficients (and this may be the appropriate route to consider if the emphasis of the student project is dimensional analysis and fluid mechanics); a basic spreadsheet can be used to compute the necessary summations.

For the case where the linear regression we seek has the form $y = a_{1*}x$, where $a_{1*} \neq a_1$, the single regression coefficient can be solved for using

$$a_1 = \frac{\sum x_i y_i}{\sum x_i^2}. \quad (\text{A12})$$

References

1. Davies, R.; Taylor, G. The mechanism of large bubbles rising through liquids in tubes. *Proc. R. Soc. Lond.* **1950**, *200A*, 375–390.
2. Zukoski, E. Influence of viscosity, surface tension, and inclination angle on motion of long bubbles in closed tubes. *J. Fluid Mech.* **1966**, *25*, 821–837. [[CrossRef](#)]
3. Whalley, P.B. Flooding, slugging, and bottle emptying. *Int. J. Multiph. Flow* **1987**, *13*, 723–728. [[CrossRef](#)]
4. Whalley, P.B. Two-phase flow during filling and emptying of bottles. *Int. J. Multiph. Flow* **1991**, *17*, 145–152. [[CrossRef](#)]
5. McQuillan, K.; Whalley, P.B. Flow patterns in vertical two-phase flow. *Int. J. Multiph. Flow* **1984**, *11*, 161–175. [[CrossRef](#)]
6. Tehrani, A.; Wragg, A.; Patrick, M. How fast will your bottle empty? *Proc. ICHEME* **1994**, 1069–1071.
7. Schmidt, O.; Kubie, J. An experimental investigation of outflow of liquids from single-outlet vessels. *Int. J. Multiph. Flow* **1995**, *21*, 1163–1168. [[CrossRef](#)]
8. Kordestani, S.; Kubie, J. Outflow of liquids from single-outlet vessels. *Int. J. Multiph. Flow* **1996**, *22*, 1023–1029. [[CrossRef](#)]
9. Tang, S.; Kubie, J. Further investigations of flow in single inlet/outlet vessels. *Int. J. Multiph. Flow* **1997**, *23*, 809–814. [[CrossRef](#)]
10. Clanet, C.; Searby, G. On the glug-glug of ideal bottles. *J. Fluid Mech.* **2004**, *510*, 145–168. [[CrossRef](#)]
11. Geiger, F.; Velten, K.; Methner, F.J. 3D CFD simulation of bottle emptying process. *J. Food Eng.* **2012**, *109*, 609–618. [[CrossRef](#)]
12. Mer, S.; Praud, O.; Neau, H.; Merigoux, N.; Magnaudet, J.; Roig, V. The emptying of a bottle as a test case for assessing interfacial momentum exchange models for Euler-Euler simulations of multi-scale gas-liquid flows. *Int. J. Multiph. Flow* **2018**, *106*, 109–124. [[CrossRef](#)]
13. Mer, S.; Praud, O.; Magnaudet, J.; Roig, V. Emptying of a bottle: How a robust pressure-driven oscillator coexists with complex two-phase flow dynamics. *Int. J. Multiph. Flow* **2019**, *118*, 23–36. [[CrossRef](#)]
14. Middleman, S. *An Introduction to Fluid Dynamics: Principles of Analysis and Design*; John Wiley & Sons: Hoboken, NJ, USA, 1998.
15. Tobin, S.; Meagher, A.; Bulfin, B.; Möbius, M.; Hutzler, S. A public study of the lifetime distribution of soap films. *Am. J. Phys.* **2011**, *79*, 819–824. [[CrossRef](#)]
16. Levine, D.; Ramsey, P.; Schmidt, R. *Applied Statistics for Engineers and Scientists*; Prentice Hall: Englewood Cliffs, NJ, USA, 2001.
17. Dunn, P. *Measurement and Data Analysis for Engineering and Science*; CRC Press: Boca Raton, FL, USA, 2010.
18. Bulmer, M. *Principles of Statistics*; Dover Publications: New York, NY, USA, 1979.
19. Walpole, R.; Myers, R. *Probability and Statistics for Engineers and Scientists*; The Macmillan Company: New York, NY, USA, 1972.
20. Figliola, R.; Beasley, D. *Theory and Design for Mechanical Measurements*; John Wiley and Sons: Hoboken, NJ, USA, 2000.
21. Montgomery, D.; Runger, G. *Applied Statistics and Probability for Engineers*; John Wiley and Sons: Hoboken, NJ, USA, 1999.

22. Naatanen, R. An explanation for differences between stop-watch and mechanical timing of races. *Percept. Mot. Skills* **1969**, *28*, 79–89. [[CrossRef](#)] [[PubMed](#)]
23. Fay, J.A. *Introduction to Fluid Mechanics*; MIT Press: Cambridge, UK, 1994.
24. Pritchard, P. *Fox and McDonald's Introduction to Fluid Mechanics*, 8th ed.; John Wiley & Sons: Hoboken, NJ, USA, 2011.
25. Faber, T.E. *Fluid Dynamics for Physicists*; Cambridge University Press: Cambridge, UK, 2004.
26. Yih, C. *Stratified Flows*; Academic Press: Cambridge, MA, USA, 1980.
27. Massey, F. The Kolmogorov–Smirnov test for goodness of fit. *J. Am. Stat. Assoc.* **1951**, *46*, 68–78. [[CrossRef](#)]



© 2019 by the author. Licensee MDPI, Basel, Switzerland. This article is an open access article distributed under the terms and conditions of the Creative Commons Attribution (CC BY) license (<http://creativecommons.org/licenses/by/4.0/>).